Dalton Transactions

PAPER

View Article Online
View Journal | View Issue

Cite this: *Dalton Trans.*, 2014, **43**, 7176

Modular syntheses of H_4octapa and H_2dedpa, and yttrium coordination chemistry relevant to $^{86}Y/^{90}Y$ radiopharmaceuticals†

Eric W. Price,[a,b] Jacqueline F. Cawthray,[a,b] Michael J. Adam[b] and Chris Orvig*[a]

The ligands H_2dedpa, H_4octapa, *p*-SCN-Bn-H_2dedpa, and *p*-SCN-Bn-H_4octapa were synthesized using a new protection chemistry approach, with labile *tert*-butyl esters replacing the previously used methyl esters as protecting groups for picolinic acid moieties. Additionally, the ligands H_2dedpa and *p*-SCN-Bn-H_2dedpa were synthesized using nosyl protection chemistry for the first time. The use of *tert*-butyl esters allows for deprotection at room temperature in trifluoroacetic acid (TFA), which compares favorably to the harsh conditions of refluxing HCl (6 M) or LiOH that were previously required for methyl ester cleavage. H_4octapa has recently been shown to be a very promising ^{111}In and ^{177}Lu ligand for radiopharmaceutical applications; therefore, coordination chemistry studies with Y^{3+} are described to assess its potential for use with $^{86}Y/^{90}Y$. The solution chemistry of H_4octapa with Y^{3+} is shown to be suitable *via* solution NMR studies of the $[Y(octapa)]^-$ complex and density functional theory (DFT) calculations of the predicted structure, suggesting properties similar to those of the analogous In^{3+} and Lu^{3+} complexes. The molecular electrostatic potential (MEP) was mapped onto the molecular surface of the DFT-calculated coordination structures, suggesting very similar and even charge distributions between both the Lu^{3+} and Y^{3+} complexes of octapa^{4-}, and coordinate structures between 8 (ligand only) and 9 (ligand and one H_2O). Potentiometric titrations determined H_4octapa to have a formation constant (log K_{ML}) with Y^{3+} of 18.3 ± 0.1, revealing high thermodynamic stability. This preliminary work suggests that H_4octapa may be a competent ligand for future $^{86}Y/^{90}Y$ radiopharmaceutical applications.

Received 22nd January 2014,
Accepted 13th March 2014

DOI: 10.1039/c4dt00239c

www.rsc.org/dalton

Introduction

When designing radiometal-based radiopharmaceuticals, an attractive feature is the ability to choose a bifunctional chelating ligand (BFC) that can effectively radiolabel with multiple different radiometals.[1] The benefit to this modular aspect of BFC-based radiopharmaceuticals is that by changing the radiometal, the same molecular construct can be used for different types of imaging and therapy, with a variety of half-lives and emission energies.[1] A radiopharmaceutical containing an appropriate BFC can be radiolabeled with an imaging isotope such as ^{111}In for pre-therapy imaging, to confirm tumor localization and calculate dosimetry. Pre-therapy imaging can then be followed with the same BFC-containing radiopharmaceutical (*e.g.* DOTA-trastuzumab), radiolabeled with a therapeutic isotope such as ^{177}Lu or ^{90}Y, to deliver a site-specific therapeutic dose.[2–4] The acyclic chelating ligand H_4octapa has demonstrated its facile radiolabeling kinetics and excellent *in vitro*/*in vivo* stability with the single photon emission computed tomography (SPECT) radiometal ^{111}In ($t_{1/2}$ ~ 2.8 days), and the β^- therapeutic radiometal ^{177}Lu ($t_{1/2}$ ~ 6.6 days).[5–9] Another attractive isotope is the β^- emitting ^{90}Y, with a shorter half-life ($t_{1/2}$ ~ 2.7 days) and higher β^- emission energy (2288 keV *vs.* 498 keV) than ^{177}Lu, allowing ^{90}Y to treat much larger and more poorly vascularized tumors (maximum *in vivo* β^- range of ~12 mm for ^{90}Y *vs.* ~2 mm ^{177}Lu).[2,3,5,10–12] The increased range of β^- particles emitted by ^{90}Y can provide therapeutic effects to neighboring tumors up to ~550 cell diameters away *via* the "crossfire effect".[2,3,5,10–12] The yttrium isotopologue ^{86}Y emits β^+ particles for positron emission tomography (PET) and is well suited for pre-therapy imaging and dosimetry. The substitution of ^{86}Y (PET) for ^{90}Y (therapy) is seamless, with the aqueous chemistry and radiolabeling properties of both isotopes of yttrium being identical; however, the nuclear properties of ^{86}Y are not ideal.[13–18] Although seemingly more attractive than ^{111}In due to its β^+ emission for PET and its identical chemistry to ^{90}Y for exchange, the serious

[a]*Medicinal Inorganic Chemistry Group, Department of Chemistry, University of British Columbia, 2036 Main Mall, Vancouver, BC V6 T 1Z1, Canada*
[b]*TRIUMF, 4004 Wesbrook Mall, Vancouver, BC V6 T 2A3, Canada.*
E-mail: orvig@chem.ubc.ca; Fax: +1(604) 822-2847; Tel: +1(604) 822-4449
† Electronic supplementary information (ESI) available: ^{1}H/^{13}C NMR spectra and FT-ATR-IR spectra of final synthesized compounds. See DOI: 10.1039/c4dt00239c

limitations of ^{86}Y include a shorter half-life (14.7 h) than the common therapeutic radiometals ^{177}Lu and ^{90}Y, high energy β^+ emission (2019, 2335 keV) that decrease image quality, and a number of high energy γ emissions (1077, 1153, 1854, 1921 keV) that present radiation dose concerns and require substantial radioactive shielding for handling and transport.[5] For these reasons, BFCs such as DOTA and CHX-A″-DTPA, which can effectively bind multiple radiometals such as ^{111}In, ^{177}Lu, and ^{86}Y/^{90}Y, are valued (Chart 1). 3p-C-NETA is a new NOTA derivative that has shown excellent properties with ^{177}Lu and ^{86}Y/^{90}Y, radiolabeling in only 5 minutes at room temperature, but its radiolabeling properties with ^{111}In are uncertain (Chart 1).[19–21]

Although excellent thermodynamic stability and kinetic inertness are crucial properties for radiometal-BFC complexes, fast radiolabeling at ambient temperature is also a very attractive property, because these radiometals are often used with antibody-based radiopharmaceuticals that are heat sensitive. H_4octapa has been shown to radiolabel with ^{111}In and ^{177}Lu in under 15 minutes at room temperature, where DOTA requires temperatures of 37–90 °C over a period of 30–60 minutes.[1,7,22–26] CHX-A″-DTPA can effectively radiolabel at ambient temperatures (30–60 min), but to achieve optimal radiolabeling yields it typically requires conditions of 37–75 °C over a period of 30–60 minutes (Chart 1).[1,7,22–26] Although the optimal radiolabeling temperatures for DOTA and CHX-A″-DTPA are high (60–100 °C), antibody-conjugates can be effectively radiolabeled at 37 °C, albeit with longer reaction times, lower yields, and typically inconsistent yields.[8] Because of its proficiency with ^{111}In and ^{177}Lu (25 °C, 15 min, >95% RCY), H_4octapa should demonstrate similarly fast radiolabeling kinetics and robust stability with ^{86}Y/^{90}Y. Towards this end, we have performed potentiometric titrations with H_4octapa and Y^{3+} to determine the thermodynamic formation constants (log K_{ML}) and pM value, and have prepared the coordination complex of H_4octapa with non-radioactive Y^{3+} to compare its properties to the previously studied complexes with In^{3+} and Lu^{3+}.[7,8] Future studies with radioactive ^{86}Y/^{90}Y will assess radiolabeling performance and *in vitro*/*in vivo* stability with H_4octapa. The current challenges facing yttrium radiochemistry are the scarce availability of ^{86}Y in North America, the non-ideal nuclear properties of ^{86}Y, and the lack of concomitant β^+/γ emissions of ^{90}Y that make detection and handling more challenging.

Antibody conjugates are large biomolecules (~150 kDa) that have long biological half-lives (~2–3 weeks), and are therefore well matched with longer-lived isotopes such ^{111}In, ^{177}Lu, and ^{90}Y.[27] Peptide conjugates typically have much faster localization and clearance times than do antibodies *in vivo*, but have still been successfully used with the above-mentioned radiometals – the octreotide-based somatostatin receptor targeting peptide-conjugates DOTA-TOC and DOTA-TATE.[11,12,23,28–35] In order to facilitate the inclusion of H_2dedpa and H_4octapa into peptide conjugates, we have developed new protection chemistry to allow them to conjugate to peptides synthesized on-resin (*e.g.* Wang resin), and deprotect under standard conditions (*e.g.* mixture of trifluoroacetic acid–dichloromethane–triisopropylsilane). Standard peptide coupling reactions of

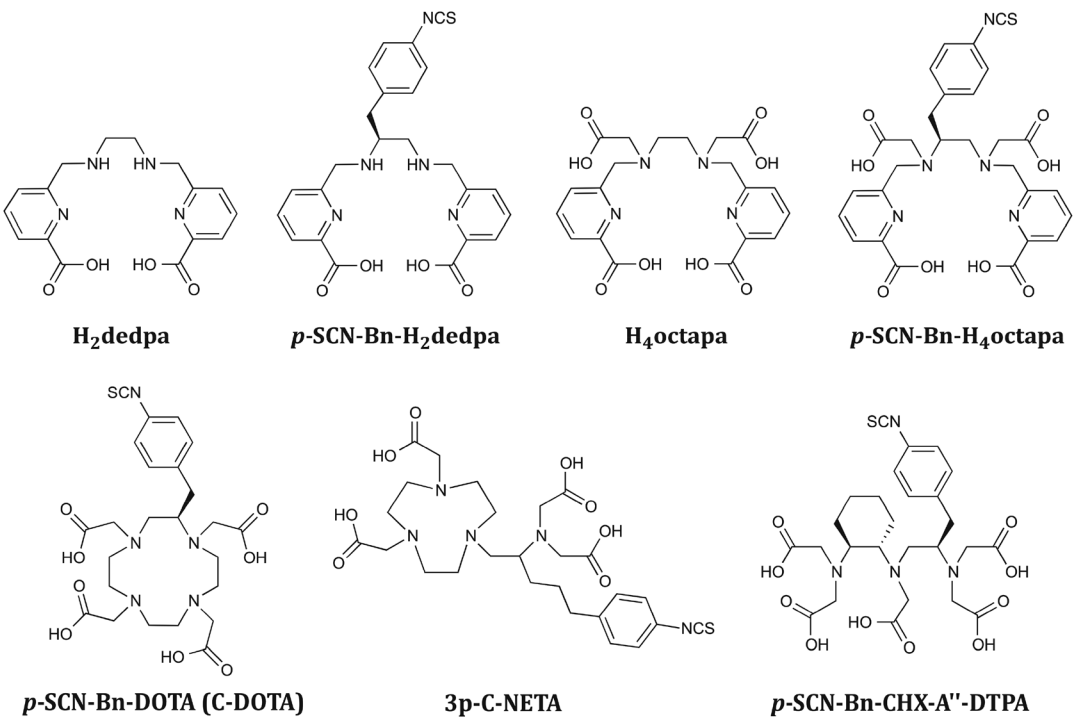

Chart 1 H_2dedpa, H_4octapa, and BFC derivatives *p*-SCN-Bn-H_2dedpa and *p*-SCN-Bn-H_4octapa; the current "gold standard" chelating ligands for ^{86}Y/^{90}Y *p*-SCN-Bn-DOTA (C-DOTA) and *p*-SCN-Bn-CHX-A″-DTPA, and the promising new ^{86}Y/^{90}Y ligand 3p-C-NETA.

these fully deprotected ligands with peptides is not possible, as the presence of **2** (H_2dedpa) or **4** (H_4octapa) free carboxylic acid groups can also form amide linkages. Previously published synthetic routes for H_2dedpa and H_4octapa have relied on methyl ester protection of the picolinic acid moiety, requiring harsh deprotection conditions of LiOH or refluxing HCl (6–12 M). By utilizing nosyl protection chemistry, we have incorporated *tert*-butyl ester protection of the picolinic acid moiety, allowing for room temperature deprotection in trifluoroacetic acid. This new synthetic route is reported for H_2dedpa, H_4octapa, *p*-SCN-Bn-H_2dedpa, and *p*-SCN-Bn-H_4octapa. The potential of the ligand H_4octapa for use with $^{86}Y/^{90}Y$ is also investigated, through formation and study of the non-radioactive $[Y(octapa)]^-$ complex, DFT calculations of the $[Y(octapa)]^-$ coordination structure and molecular electrostatic potential (MEP), and potentiometric titrations of H_4octapa with Y^{3+} to determine its solution thermodynamic stability parameters (pM, log K_{ML}).

Results and discussion

Synthesis and characterization

Previously, only methyl-ester protection chemistry was compatible with the picolinic acid moiety of the "pa" family of ligands (Chart 1), and attempts to utilize *tert*-butyl esters had failed due to incompatibility with reductive amination methods.[36] The commercially available starting material 6-methylpicolinic acid was *tert*-butyl ester protected following a modified literature procedure, which utilized *tert*-butyl-2,2,2-trichloroacetimidate (Scheme 1).[37] The *tert*-butyl protected product (**1**) was synthesized here for the first time, and then transformed to the alkyl-bromide derivative (**2**) using a modified literature procedure with *N*-bromosuccinimide and benzoyl peroxide as radical initiator.[38] The general synthetic scheme relies heavily on the nosyl protection group, and follows the same general pathway as the recently published nosyl-based synthesis of *p*-SCN-Bn-H_4octapa.[8,9] The enhanced

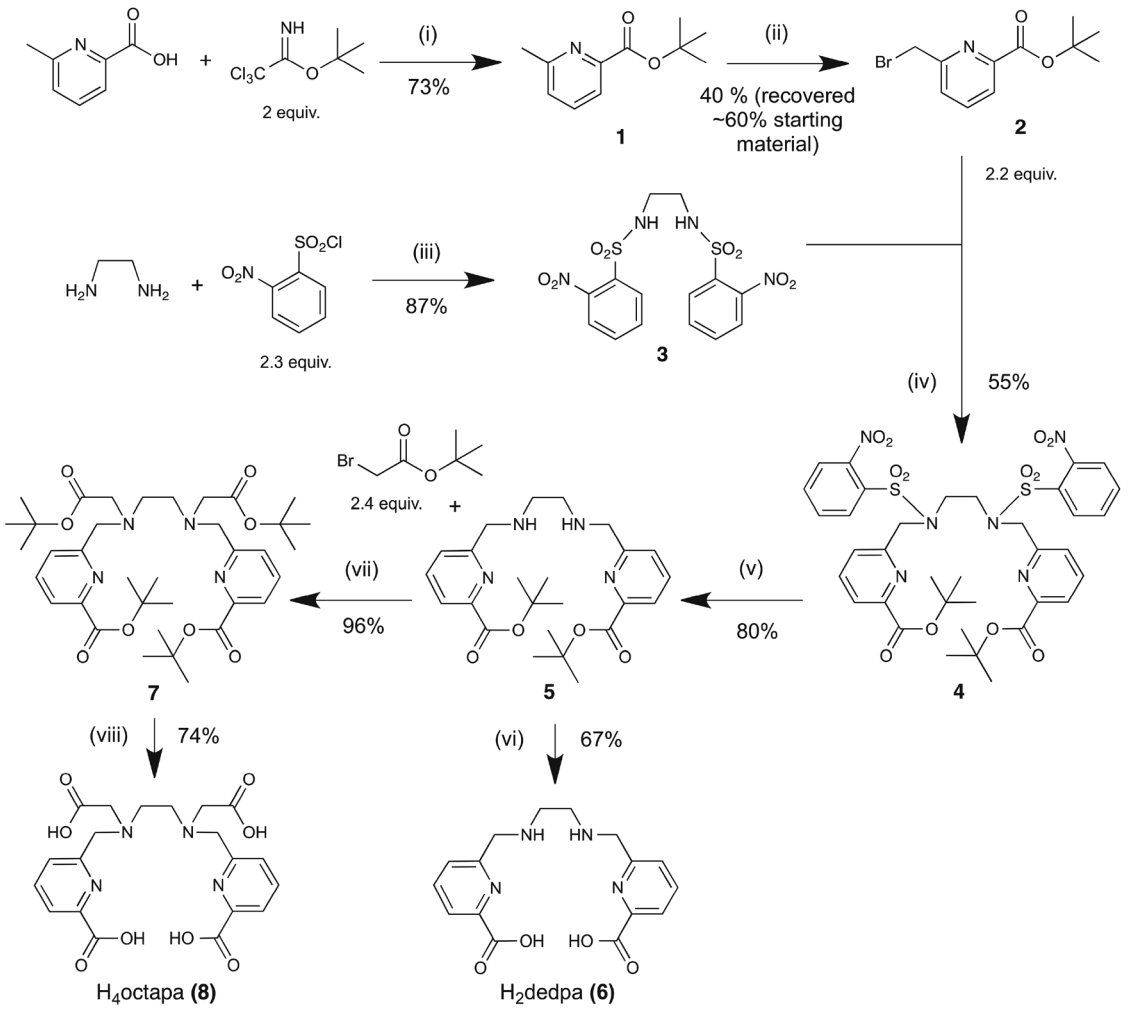

Scheme 1 Syntheses of H_2dedpa (6) and H_4octapa (8) using *tert*-butyl ester protection chemistry. (i) CH_2Cl_2, BF_3·etherate (20 μL mmol^{-1} starting material), RT, 20 h; (ii) CCl_4, Bz_2O_2, *N*-bromosuccinimide (NBS, 0.7 equiv.), 70 °C, 4 h; (iii) THF, $NaHCO_3$, RT, 24 h; (iv) DMF, Na_2CO_3, 80 °C, 48 h; (v) THF, thiophenol (2.3 equiv.), K_2CO_3, 50 °C, 48 h; (vi) trifluoroacetic acid (TFA) (1 mL) and CH_2Cl_2 (1 mL), RT, 16 h, (cumulative yield of ~26% over 4 steps); (vii) MeCN, Na_2CO_3, 60 °C, 48 h; (viii) trifluoroacetic acid (TFA) (1 mL) and CH_2Cl_2 (1 mL), RT, 16 h (cumulative yield of ~27% over 5 steps).

lability of the *tert*-butyl ester protecting group resulted in some decomposition during synthesis, which was partially responsible for decreased yields relative to the analogous methyl ester-based synthetic route.[6–8] Additionally, the solvent methanol was problematic, as during silica column chromatography some methyl ester product was formed from the *tert*-butyl ester, creating byproducts and decreasing yields. Because the combination of methanol and dichloromethane was most effective for separating intermediates *via* column chromatography, it was still used; however, methanol was avoided whenever possible, such as when rinsing, filtering, rotary evaporating, and heating. The previously used synthetic protocols for H_2dedpa relied upon a reductive amination reaction, which utilized $NaBH_4$ to reduce the Schiff-base (imine) to a secondary amine.[36,39–43] This method produced byproducts at the methyl ester protected picolinic acid moiety by transforming them to a mixture of carboxylic acids and primary alcohols, but for the more labile *tert*-butyl ester protection group complete ester cleavage and reduction to primary alcohols was observed, and no product could be isolated.[7] It has not been until our recent implementation of nosyl protection chemistry for the synthesis of these ligands that implementation of *tert*-butyl ester protection chemistry could be realized.[8]

An important deviation of the synthetic pathway reported here from the previously published nosyl-based synthesis of *p*-SCN-Bn-H_4octapa is the enhanced modularity, with the *tert*-butyl ester protected precursors (tBu)$_2$dedpa (**5**) and *p*-NO_2-Bn-(tBu)$_2$dedpa (**13**) being arranged as precursors to (tBu)$_4$octapa (**7**) and *p*-NO_2-Bn-(tBu)$_4$octapa (**15**) (Schemes 1 and 2). Using this layout, common synthetic precursors are used for both

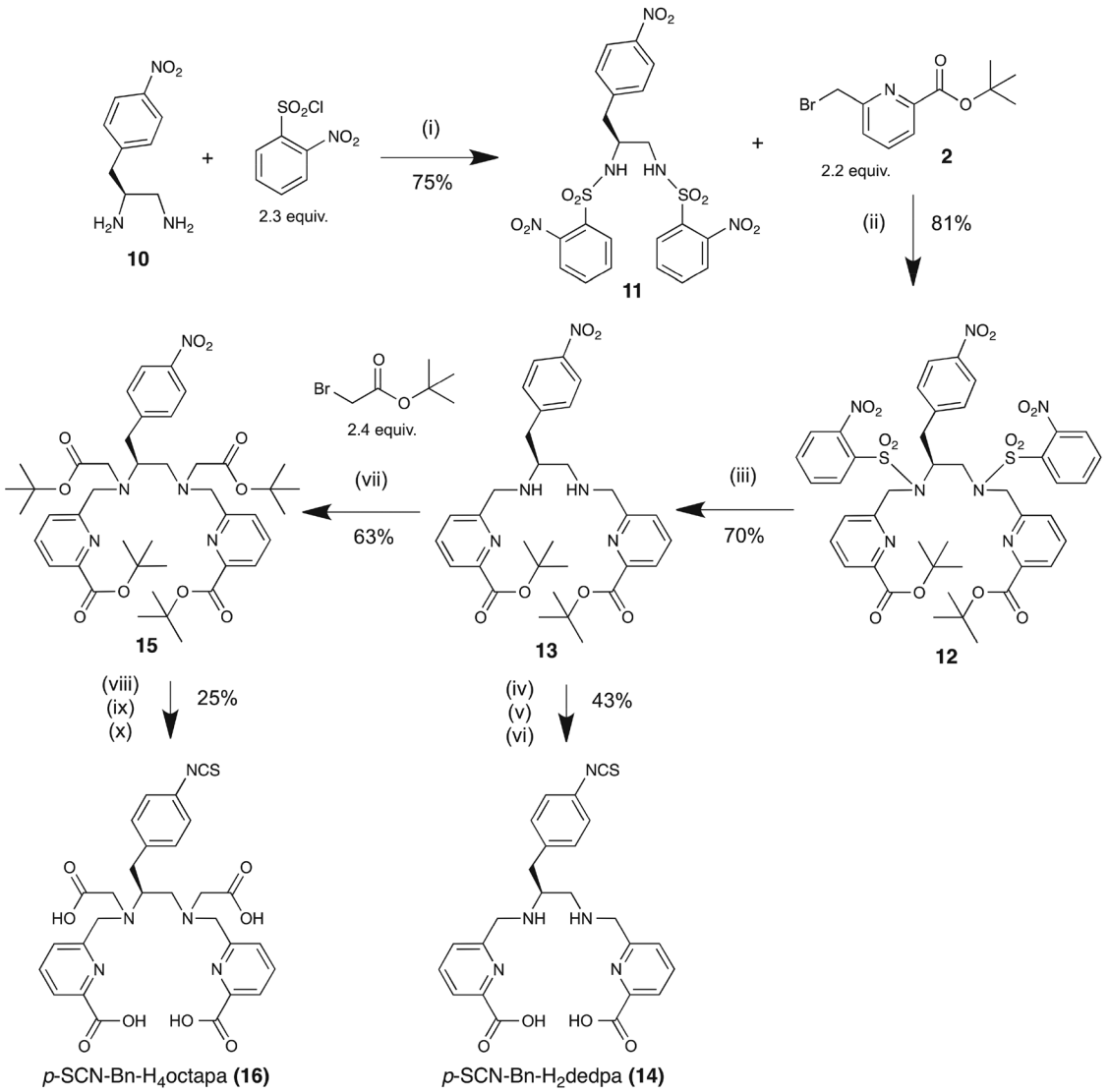

Scheme 2 Synthesis of *p*-SCN-Bn-H_2dedpa (14), and *p*-SCN-Bn-H_4octapa (16) using *tert*-butyl ester protection chemistry. (i) THF, $NaHCO_3$, 50 °C, 24 h; (ii) DMF, Na_2CO_3, 80 °C, 48 h; (iii) THF, thiophenol (2.3 equiv.), K_2CO_3, 60 °C, 48 h; (iv) 5 mL of (1 : 1) glacial acetic acid : 3 M HCl, Pd/C (20 wt%), H_2 (g), RT, 1 h; (v) 3 M HCl, heat to reflux for 1 minute; (vi) thiophosgene in DCM (15 equiv.), 3 M HCl, RT, 24 h (cumulative yield of ~18% in 6 steps); (vii) MeCN, K_2CO_3, 80 °C, 48 h; (viii) 5 mL of (1 : 1) glacial acetic acid : 3 M HCl, Pd/C (30 wt%), H_2 (g), RT, 1 h; (ix) 3 M HCl, heat to reflux for 1 minute; (x) thiophosgene in DCM (15 equiv.), 3 M HCl, RT, 24 h (cumulative yield of ~7% in 7 steps).

H_2dedpa and H_4octapa, rendering the reaction schemes nearly identical for each. The utility of this approach is that the ^{64}Cu and ^{67}Ga/^{68}Ga ligand H_2dedpa can be made in the same procedure as the ^{111}In, ^{177}Lu, and ^{86}Y/^{90}Y ligand H_4octapa, sharing common precursors and resulting in broad radiometal application from one synthetic scheme. Previously, in order to optimize purification and yields, *p*-SCN-Bn-H_4octapa was synthesized using a different reaction ordering that did not allow for this overlap.[8] Despite this alternate approach, the same reaction pathways (Schemes 1 and 2) can be performed using the previously published methyl ester protected picolinic acid group instead of its *tert*-butyl protected analogue. The drawback to the methyl ester protected picolinic acid moiety lies in the purification of the $(Me)_2$dedpa intermediate, which is more challenging than the more lipophilic $(t$Bu$)_2$dedpa derivative; however, the enhanced stability of the methyl ester protection group affords higher yields, at the price of harsh deprotection conditions.[7,8,36] H_2dedpa and H_4octapa have previously been synthesized as HCl salts, but for this new synthesis they were lyophilized after final high-performance liquid chromatography (HPLC) purification as their trifluoroacetic acid salts. The final trifluoroacetic acid salts (formulae determined from elemental analysis results) H_2dedpa·2trifluoroacetic acid·1.5H_2O and H_4octapa·2trifluoroacetic acid were more soluble in water than their HCl counterparts, and were now soluble in methanol.

During the syntheses of the bifunctional derivatives *p*-SCN-Bn-H_2dedpa (**14**) and *p*-SCN-Bn-H_4octapa (**16**), it was observed that the hydrogenation reaction conditions used with the precursors *p*-NO_2-Bn-$(t$Bu$)_2$dedpa (**13**) and *p*-NO_2-Bn-$(t$Bu$)_4$octapa (**15**) surprisingly did not effect full *tert*-butyl ester deprotection. The hydrogenation was performed using 1 : 1 glacial acetic acid and hydrochloric acid (3 M) as solvent at room temperature for 1 hour, and mass spectrometry confirmed that *p*-NH_2-Bn-$(t$Bu$)_2$dedpa (not isolated, used without further purification) was formed without *tert*-butyl ester cleavage. Mass spectrometry suggested that *p*-NH_2-Bn-$(t$Bu$)_2H_2$-octapa was formed after hydrogenation, with two *tert*-butyl ester groups being cleaved and two remaining attached; however, this intermediate was not isolated and was used without further purification. Full deprotection of these intermediates was performed after isothiocyanate formation.

H_2dedpa (**6**) was synthesized in 4 synthetic steps and H_4octapa (**8**) in 5 steps, with cumulative yields of ~26% and ~27%, respectively. The more synthetically challenging bifunctional derivative *p*-SCN-Bn-H_2dedpa (**14**) was synthesized in 6 steps and *p*-SCN-Bn-H_4octapa (**16**) in 7 steps, with cumulative yields of ~18% and ~7%, respectively. The previously reported nosyl-based synthesis of H_4octapa and *p*-SCN-Bn-H_4octapa that utilized methyl ester protection chemistry of the picolinic acid moieties were produced in higher cumulative yields of ~45–50% and ~25–30%, respectively.[8] H_2dedpa (**6**) and *p*-SCN-Bn-H_2dedpa (**14**) have not been previously synthesized using nosyl protection chemistry, and are reported here for the first time. Largely due to the enhanced lability of the *tert*-butyl ester protected picolinic acid, a penalty in cumulative yield was paid for access to less harsh room temperature deprotection in trifluoroacetic acid. Synthesis of *p*-SCN-Bn-$(t$Bu$)_2$dedpa or *p*-NH_2-Bn-$(t$Bu$)_2$dedpa for direct conjugation to on-resin peptides should afford easy purification and high yields, which was not previously possible using the methyl ester protected derivative.

Yttrium coordination chemistry and density functional theory/molecular electrostatic potential structure prediction

The Y^{3+} complex of H_4octapa, $[Y(octapa)]^-$ (**9**), was synthesized by mixing **8** (H_4octapa·2trifluoroacetic acid) with $YCl_3·6H_2O$ in deionized water, adjusting the pH to ~4–5 with NaOH (0.1 M), and stirring at room temperature for 1 hour. After confirming formation of the coordination complex by mass spectrometry, the product was studied by NMR in both D_2O and DMSO-d_6 (Fig. 1, Fig. S32†). The same $[Y(octapa)]^-$ NMR sample was run

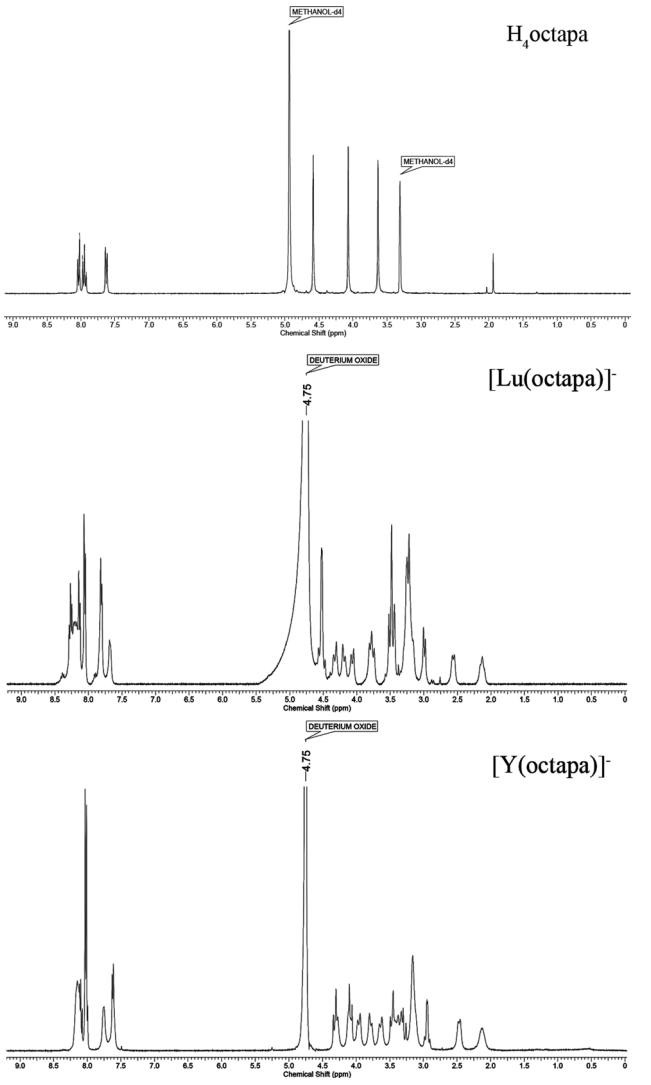

Fig. 1 ^{1}H NMR spectra of H_4octapa (400 MHz, 25 °C, top, referenced to H-O-D at 4.75 ppm), $[Lu(octapa)]^-$ in D_2O (600 MHz, 25 °C, middle),[8] and $[Y(octapa)]^-$ in D_2O (400 MHz, 25 °C, bottom) showing the ^{1}H NMR splitting patterns in the D_2O spectra of the Y^{3+} and Lu^{3+} complexes to be similar, suggesting that they may possess similar solution structures and coordination numbers (*e.g.* a mixture of static and fluxional isomers, *vide infra*).

repeatedly over a period of 3–4 weeks (*e.g.* ^{1}H, ^{13}C, VT, 2D NMR) with no discernable changes observed in the acquired spectra, suggestion that equilibrium was reached quickly. A comparison of the ^{1}H NMR spectra of [Lu(octapa)]$^{-}$ (Fig. 1, middle) and [Y(octapa)]$^{-}$ (Fig. 1, bottom) in D_2O reveals similarly sharp signals and coupling patterns, but slightly different chemical shift values, suggesting similar solution structures.[8] Different absolute chemical shift values are expected, as Y^{3+} and Lu^{3+} have different electronic properties, but these two metal ions are known to form coordination structures with similar geometries (CN = 8–9), as they both have similar ionic radii (CN = 8, 101.9 pm *vs.* 97.7 pm, and CN = 9, 107.4 pm *vs.* 103.2 pm, respectively).[44] At first glance, the sharp and well-resolved peaks and couplings observed for both the Y^{3+} and Lu^{3+} complexes of octapa^{4-} suggest little fluxional behavior in solution at 25 °C, but the large number of signals and complicated coupling patterns relative to the simple ^{1}H NMR spectra of [In(octapa)]$^{-}$ and the unbound ligand H_4octapa suggest the presence of multiple static isomers (Fig. 1).[7] In addition to multiple geometric isomers, it is possible that upon coordination of a single water molecule to the [Y(octapa)]$^{-}$ complex, the 9-coordinate [Y(octapa)(H_2O)]$^{-}$ geometry is lower symmetry giving a greater number of non-equivalent protons and a more complicated spectrum. The NMR spectrum of [Y(octapa)]$^{-}$ in DMSO-d_6 was significantly different than in D_2O, potentially as a result of coordination of DMSO to Y^{3+} (Fig. S32†). The increased broadening of NMR signals (Fig. S32†) in DMSO-d_6 also suggests an increased rate of fluxional isomerization.

To further probe the coordination structure and isomerization of the [Y(octapa)]$^{-}$ complex, variable temperature-NMR (VT-NMR) and 2D-COSY/HSQC experiments were performed. Upon increasing the NMR sample (D_2O) temperature from 25 °C to 85 °C, the multiple sharp peaks observed in the 25 °C spectrum did not change drastically, which suggests the presence of a stable static isomer (red arrows, Fig. 2). For the broad signals observed at 25 °C (blue arrows, Fig. 2), substantial change in the ^{1}H NMR spectrum was observed after a small change in temperature between 25 °C and 45 °C, with some signals broadening to such an extent that they nearly disappeared from the spectrum. This trend of broadening and coalescing of signals continued up to 85 °C; however, even at 85 °C some signals remained sharp. It can be seen in Fig. 2 that some sharp signals remain the same between 25 °C and 45 °C (red arrows), where other more broad signals that overlap these sharp signals are observed to rapidly broaden and coalesce (blue arrows). This observation suggests that a single major static isomer is present in solution (red arrows, sharp peaks that remain as temperature is increased), with at least one fluxional isomer existing at the same time (blue arrows). The signals highlighted by red arrows (Fig. 2) resemble the more simple spectra obtained previously for [In(octapa)]$^{-}$, where only a single static isomer was present, with several doublets and simple multiplets arising from neighboring protons on the H_4octapa scaffold becoming diastereotopic upon In^{3+} coordination, and coupling to each other.[7] Because yttrium can form 9-coordinate complexes, the coordination of an aqua ligand could be involved in the fluxional isomerization of [Y(octapa)]$^{-}$. These VT-NMR experiments suggest that one static isomer and at least one set of fluxional isomers are present under aqueous conditions at ambient temperature, with the fluxional species rapidly broadening upon heating, and the static isomer changing very little upon heating (Fig. 2).

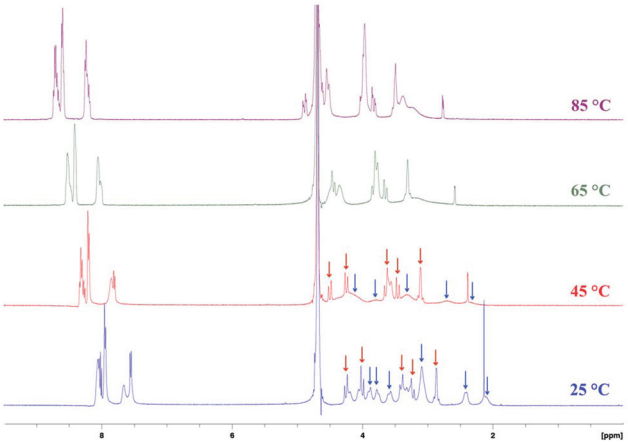

Fig. 2 Variable temperature (VT) NMR experiments with [Y(octapa)]$^{-}$ (D_2O, 400 MHz), showing a mixture of sharp signals and broad signals at 25 °C, with the broad signals rapidly changing and beginning to coalesce as the temperature was increased to 85 °C in 20 °C increments (blue arrows), suggesting these signals arise from fluxional isomers, and the sharp signals (red arrows) changing very little upon increased temperature, suggesting these signals arise from a stable static isomer.

The 2D-COSY experiment was used to probe ^{1}H–^{1}H correlations, to see if distinct static isomers could be observed at ambient temperature and confirm VT NMR results (Fig. 3 and 4). An expansion of the aromatic region of the 2D-COSY spectrum revealed strongly correlated cross-peaks between the sharp signals, which were attributed to a single major static isomer in solution (Fig. 3). Additionally, weak cross-peaks

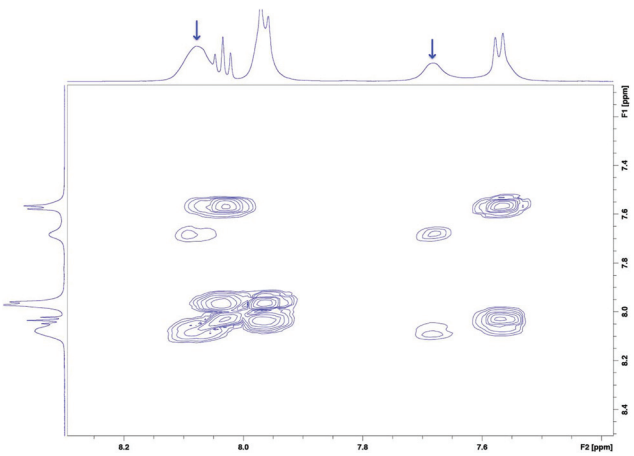

Fig. 3 ^{1}H–^{1}H COSY NMR (600 MHz, D_2O, 25 °C) expansion of aromatic signals in the spectrum of [Y(octapa)]$^{-}$, showing no correlations between broad signals arising from a fluxional species (blue arrows), and sharp signals arising from a single static isomer (see Fig. S32† for full spectrum).

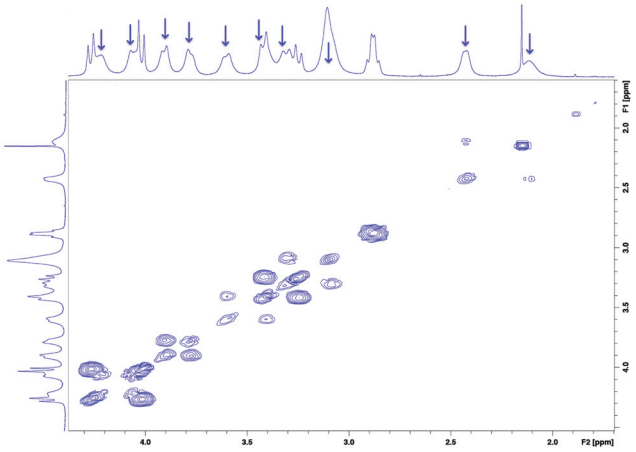

Fig. 4 $^{1}H–^{1}H$ COSY NMR (600 MHz, D_2O, 25 °C) expansion of alkyl signals in the spectrum of $[Y(octapa)]^-$, showing no correlations between broad signals arising from a fluxional species (blue arrows, identified by VT-NMR, Fig. 2), and sharp signals arising from a single static isomer (see Fig. S32† for full spectrum).

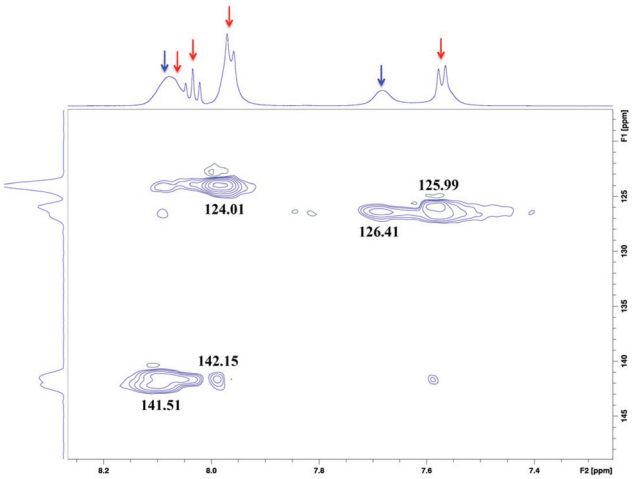

Fig. 5 $^{1}H–^{13}C$ HSQC NMR (400/100 MHz, D_2O, 25 °C) expansion of aromatic signals in the spectrum of $[Y(octapa)]^-$, showing correlations to ~5 unique ^{13}C signals, suggesting the presence of a single static isomer (red arrows), along with a fluxional species (blue arrows) (^{13}C NMR spectra externally referenced to MeOH in D_2O) (see Fig. S33† for full spectrum).

between the broad signals that were assigned as a fluxional isomer in VT NMR experiments (blue arrows, Fig. 3) were observed, and showed no correlation to the sharp signals. The same conclusion can be drawn from the COSY alkyl-region expansion (blue arrows, Fig. 4), where the broad signals which were observed to rapidly disappear after the temperature was increased during VT-NMR experiments (Fig. 2), can now be seen to weakly correlate which each other, and further to show no correlation with the sharp signals assigned as the major static isomer. These 2D-NMR experiments confirm the results of the VT-NMR experiments, suggesting the presence of one major static isomer in solution, along with at least one fluxional species. Fluxional species typically produce very weak NMR data, demonstrated by weak cross peaks correlating to a fluxional species in the 2D COSY experiments discussed above (Fig. 3 and 4), and strong cross peaks correlating to the major static isomer.

Because 2D-HSQC experiments utilize $^{1}H–^{13}C$ heteronuclear correlations, the signals obtained for fluxional species are even weaker than those for the COSY spectra, as they rely on ^{13}C NMR data collection as well as ^{1}H NMR. The 2D-HSQC $^{1}H–^{13}C$ single-bond heteronuclear correlation experiment revealed a strong set of cross-peaks arising from a single static isomer (red arrows, Fig. 5), with only weak signals and cross-peaks arising from the observed fluxional species (blue arrows, Fig. 5). For the unbound and symmetric ligand H_4octapa, one would expect to see 3 distinct aromatic ^{13}C signals arising from the three distinct C–H pyridines ($\sim C_{2v}$ symmetry), and for a single static isomer of $[Y(octapa)]^-$ there would be 3–6 signals (depending on symmetry). It was observed that the aromatic region of the $[Y(octapa)]^-$ HSQC NMR spectrum displayed ~5 unique and strong ^{13}C correlation signals, supporting the hypothesis of a single major static isomer (Fig. 5). There are 6 unique alkyl-carbon atoms present in H_4octapa/$[Y(octapa)]^-$, which manifest as 3 sharp signals for the free H_4octapa ligand (Fig. 1, top). Expansion of the alkyl region of the HSQC NMR spectrum revealed strong correlations to ~4 unique carbon atoms (red arrows, Fig. 6), with many weaker signals likely corresponding to the fluxional species (blue arrows, Fig. 6), again suggesting the presence of a single major static isomer of $[Y(octapa)]^-$, along with a fluxional species. Because yttrium typically forms 8–9 coordinate complexes, there is likely a mixture of $[Y(octapa)]^-$ and $[Y(octapa)(H_2O)]^-$, with the single aqua ligand potentially exchanging in solution and producing the observed fluxional species. It is unclear if these two isomers are a mixture

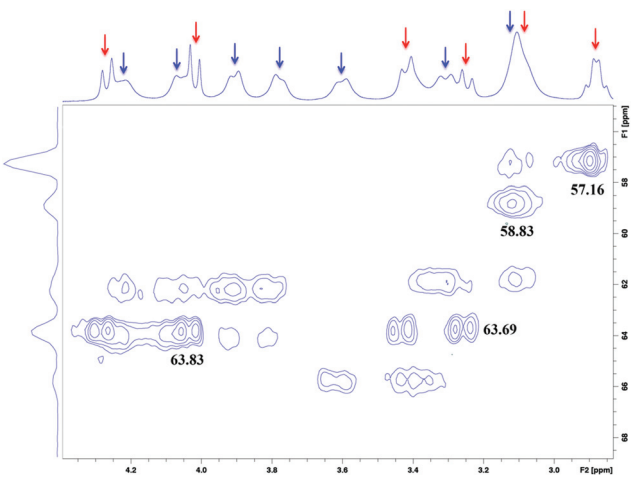

Fig. 6 $^{1}H–^{13}C$ HSQC NMR (400/100 MHz, D_2O, 25 °C) expansion of alkyl-region signals in the spectrum of $[Y(octapa)]^-$, showing correlations to ~4 unique and strong ^{13}C signals (red arrows), suggesting the presence of 1 static isomer, along with several weak correlations arising from a fluxional species (blue arrows) (^{13}C NMR spectra externally referenced to MeOH in D_2O) (see Fig. S33† for full spectrum).

between [Y(octapa)]$^-$ and [Y(octapa)(H$_2$O)]$^-$, or different geometric isomers. RP-HPLC purification (no buffer, deionized water and acetonitrile) of [Y(octapa)]$^-$ revealed a single broad peak, as is typically observed for all H$_2$dedpa/H$_4$octapa free ligands and metal complexes to date, suggesting that the two isomers have similar or identical physical properties (*e.g.* polarity) (Fig. S34†). These VT-NMR and 2D-NMR studies have not been performed on the [Lu(octapa)]$^-$ complex, but the similarities between their basic ^{1}H-NMR spectra (Fig. 1) would suggest that [Lu(octapa)]$^-$ also exists in solution as a mixture of a single static isomer and a fluxional species.

It is difficult to draw concrete conclusions, but these NMR studies suggest that [Y(octapa)]$^-$ is present as a mixture of a single major isomer and a fluxional species. The NMR sample of [Y(octapa)]$^-$ (D$_2$O) was run repeatedly over a period of 3–4 weeks with no changes, suggesting that equilibrium was reached rapidly. These isomers could not be separated by RP-HPLC (Fig. S34†). It is important to note that these NMR solution studies cannot be used to predict *in vivo* kinetic stability, and radiochemical experiments (*e.g. in vitro* serum stability and *in vivo* biodistribution studies with ^{86}Y/^{90}Y) must be performed.

Coordination geometries were calculated by density functional theory (DFT) calculations for both the binary 8-coordinate [Y(octapa)]$^-$ (Fig. 7a) complex and the 9-coordinate monohydrate [Y(octapa)(H$_2$O)]$^-$ (Fig. 7b), as yttrium can form either 8- or 9-coordinate complexes in solution. The DFT structures of the complexes [Lu(octapa)]$^-$, [Lu(octapa)(H$_2$O)]$^-$, and [In(octapa)]$^-$ have been calculated and studied previously.[7,8] The molecular electrostatic potential (MEP) surfaces shown in Fig. 7 (bottom) show very similar charge distributions between the 8- or 9-coordinate complexes of octapa^{4-} with Y^{3+}, and are very similar to those calculated for the Lu^{3+} and In^{3+} complexes.[7,8] These observations suggest that the solution behavior of the coordination complexes of octapa^{4-} with Lu^{3+} and Y^{3+} may be very similar, with both metal complexes having the same overall 1$^-$ charge and nearly identical charge distributions as predicted by DFT/MEP calculations, foreshadowing both metal complexes to share *in vivo* properties.

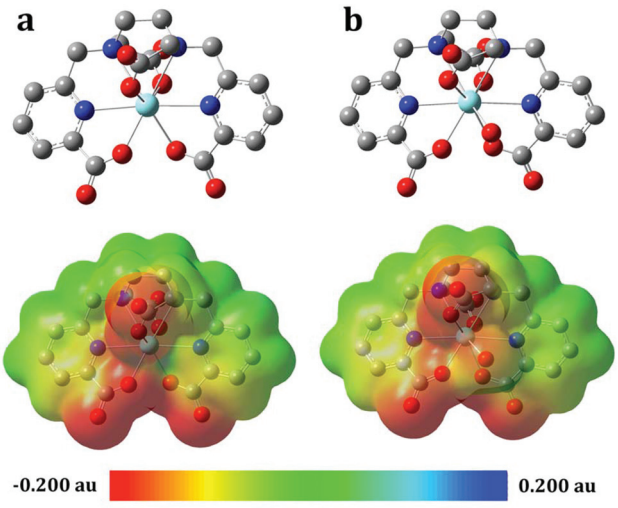

Fig. 7 *In silico* DFT structure predictions: (a) 8-coordinate structure of [Y(octapa)]$^-$ (top, left); (b) 9-coordinate structure of [Y(octapa)(H$_2$O)]$^-$ (top, right), as well as the MEP polar-surface area maps (bottom) predicting the charge distribution over the solvent-exposed surface of the metal complexes (red = negative, blue = positive, representing a maximum potential of 0.200 au and a minimum of −0.200 au, mapped onto electron density isosurfaces of 0.002 Å^{-3}), demonstrating very little difference between the 8- and 9-coordinate solution structures in terms of both geometry and charge distribution, suggesting little change in physical properties between the 8- and 9-coordinate geometries.

Thermodynamic stability

The ligands H$_2$dedpa and H$_4$octapa have previously been evaluated with a number of metal ions, including Cu^{2+}, Ga^{3+}, In^{3+}, and Lu^{3+}.[7,8,36,39,40] Recently, H$_4$octapa has been found to have exceptional radiolabeling properties with ^{111}In and ^{177}Lu, and has shown very promising *in vivo* behavior when compared to the industry "gold standards" DTPA and DOTA.[7,8] Thermodynamic stability constants for the ligands H$_2$dedpa, H$_4$octapa, DTPA, and DOTA, with the metal ions In^{3+}, Lu^{3+}, and Y^{3+} are shown in Table 1. The formation constant (log K_{ML}) and pM value for H$_4$octapa with Y^{3+} has been experimentally determined for the first time using EDTA competition potentiometric titrations. The pM (−log[M]) value is a condition-dependent thermodynamic parameter ([M] = 1 μM, [L] = 10 μM, pH 7.4, 25 °C) that is considered more biologically relevant than log K_{ML} values, as it additionally takes into account conditions such as ligand basicity, metal ion hydrolysis, physiological pH, and ligand : metal ratio.[45–48] As previously determined, H$_4$octapa has been shown to possess exceptionally high log K_{ML} and pM values with In^{3+} and Lu^{3+}, with pM values exceeding those of the ligands DTPA and DOTA (Table 1). The log K_{ML} value for H$_4$octapa with Y^{3+} has been experimentally determined here to be 18.3 ± 0.1 (pM = 18.1) (Table 1). A comparison of the thermodynamic stability constant of H$_4$octapa to other ligands with Y^{3+} shows the log

Table 1 Formation constants (log K_{ML}) and pM[a] values for In^{3+}, Lu^{3+}, and Y^{3+} complexes of relevant chelating ligand

Ligand	M^{3+}	log K_{ML}	pM[a]	Ref.
dedpa^{2-}	In^{3+}	26.60(4)	25.9	7
octapa^{4-}	In^{3+}	26.8(1)	26.5	7
	Lu^{3+}	20.08(9)	19.8	8
	Y^{3+}	18.3(1)	18.1	
DTPA^{4-}	In^{3+}	29.0	25.7	51, 53
	Lu^{3+}	22.6	19.1	8, 51
	Y^{3+}	21.2, 21.9, 22.5	17.6–18.3[b]	49, 50
DOTA^{4-}	In^{3+}	23.9(1)	18.8	45, 51
	Lu^{3+}	21.6(1), 23.6, 25, 29.2	17.1	8, 54–56
	Y^{3+}	24.3, 24.4, 24.9	19.3–19.8[b]	49, 50, 57
Transferrin	In^{3+}	18.3	18.7	58
	Lu^{3+}	11.08	—	59

[a] Calculated for 10 μM total ligand and 1 μM total [M^{3+}] at pH 7.4 and 25 °C. [b] pM values for DTPA and DOTA with Y^{3+} were calculated for this work, based upon previously determined log K_{ML},[49] ligand pK_a,[50,51] and metal ion pK_a values.[52]

K_{ML} value to be similar to DTPA, but lower than the current "gold standard" DOTA (Table 1). Values of pM were not available for DTPA and DOTA from the literature, and so values were calculated based on previously determined log K_{ML},[49] ligand pK_a,[50,51] and metal pK_a values.[52] From a range of log K_{ML} values that have been published for DTPA (21.2, 21.9) and DOTA (24.4, 24.9), pM values were calculated to be 17.6–18.3 (DTPA) and 19.3–19.8 (DOTA) (Table 1). Although thermodynamic parameters are very valuable, the *in vivo* stability (kinetic inertness/stability at high dilution *in vivo*) is the most important factor for determining the usefulness of radiometal complexes, as thermodynamic stability may not correlate to *in vivo* stability. To this end, serum stability assays and studies in mice must be performed in the future with the $^{86}Y/^{90}Y$ complexes of H_4octapa to properly assess the potential utility for radiopharmaceutical applications.

Conclusions

The ligands H_2dedpa, H_4octapa, *p*-SCN-Bn-H_2dedpa, and *p*-SCN-Bn-H_4octapa were synthesized using a new *tert*-butyl ester protection group scheme, allowing for deprotection at room temperature in TFA, which compares favorably to the harsh conditions of refluxing HCl (6–12 M) or LiOH that were previously required for methyl ester cleavage. Additionally, the ligands H_2dedpa and *p*-SCN-Bn-H_2dedpa were synthesized using nosyl protection chemistry for the first time. The less harsh deprotection conditions afforded by the *tert*-butyl ester groups may allow these ligands to be incorporated into sensitive molecular scaffolds in the future, such as peptides synthesized on-resin (*e.g.* Wang resin), accommodating the standard deprotection conditions of a mixture of trifluoroacetic acid, dichloromethane, and triisopropylsilane. H_4octapa has been recently shown to be a very promising ^{111}In and ^{177}Lu ligand for radiopharmaceutical applications, and density functional theory (DFT) calculations of the predicted structures of H_4octapa with Y^{3+}, In^{3+} and Lu^{3+} look similar. Potentiometric titrations have determined H_4octapa to have a formation constant (log K_{ML}) with Y^{3+} of 18.3 ± 0.1 (pM = 18.1), revealing high thermodynamic stability. These results suggest that along with ^{111}In and ^{177}Lu, H_4octapa may be a competent ligand for $^{86}Y/^{90}Y$ radiopharmaceutical applications.

Experimental

General remarks

All solvents and reagents were purchased from commercial suppliers (Sigma Aldrich, St. Louis, MO; TCI America, Portland, OR; Fisher Scientific, Waltham, MA) and were used as received unless otherwise indicated. Methyl-6-bromomethylpicolinate was synthesized according to a literature protocol.[7] Water used was ultra-pure (18.2 MΩ cm^{-1} at 25 °C, Milli-Q, Millipore, Billerica, MA). The analytical thin-layer chromatography (TLC) plates were aluminum-backed ultrapure silica gel (Siliaplate™, 60 Å pore size, 250 μM plate thickness, Silicycle, Quebec, QC). Flash column silica gel was purchased from Silicycle (Siliaflash® Irregular Silica Gels F60, 60 Å pore size, 40–63 mm particle size, Silicycle, Quebec, QC). Automated column chromatography was performed using a Teledyne Isco (Lincoln, NE) CombiFlash® R_f automated system with solid load cartridges packed with flash column silica gel and RediSep R_f Gold® reusable normal-phase silica columns and neutral alumina columns (Teledyne Isco, Lincoln, NE). ^1H and ^{13}C NMR spectra were recorded on Bruker AV300, AV400, or AV600 instruments; all spectra were internally referenced to residual solvent peaks except for ^{13}C NMR spectra in D_2O, which were externally referenced to a sample of CH_3OH–D_2O. Low-resolution mass spectrometry was performed using a Waters liquid chromatography-mass spectrometer (LC-MS) consisting of a Waters ZQ quadrupole spectrometer equipped with an ESCI electrospray/chemical ionization ion source and a Waters 2695 HPLC system (Waters, Milford, MA). High-resolution electrospray-ionization mass spectrometry (EI-MS) was performed on a Waters Micromass LCT time of flight instrument. Microanalyses for C, H, N were performed on a Carlo Erba EA 1108 elemental analyzer. The HPLC system used for purification of compounds consisted of a semi-preparative reverse phase C18 Phenomenex Synergi hydro-RP (80 Å pore size, 250 × 21.2 mm, Phenomenex, Torrance, CA) column connected to a Waters 600 controller, a Waters 2487 dual wavelength absorbance detector, and a Waters delta 600 pump.

***tert*-Butyl 6-(methyl)picolinate (1).** Commercially available 6-methylpicolinic acid (15.00 g, 109.38 mmol) was suspended in CH_2Cl_2 (500 mL). To the reaction mixture was added *tert*-butyl-2,2,2-trichloroacetimidate (47.80 g, 218.8 mmol), followed by BF_3·etherate (20 μL $mmol^{-1}$ of starting material, ~2.19 mL), and the mixture was stirred overnight at ambient temperature. The reaction mixture volume was reduced *in vacuo* to ~100 mL; the resulting white solid was filtered through a fritted glass filter and discarded, and the filtrate reduced to dryness *in vacuo*. The crude product was then resuspended in hexanes (~50 mL) and filtered again to remove additional white precipitate (unreacted *tert*-butyl-2,2,2-trichloroacetimidate, visualized by ninhydrin staining of TLC plates). The crude product was purified by silica chromatography (CombiFlash R_f automated column system; 80 g HP silica; A: CH_2Cl_2, B: MeOH, 100% A to 95% A gradient) to yield product **1** as a clear colourless oil, which later solidified into a off-white wax (73%, ~15.4 g) (R_f: 0.6, TLC in 95% CH_2Cl_2: 5% MeOH). ^1H NMR (400 MHz, $CDCl_3$, 25 °C) δ: 7.75 (d, J = 7.8 Hz, 1H), 7.60 (t, J = 7.7 Hz, 1H), 7.21 (d, J = 7.9 Hz, 1H), 2.56 (s, 3H), 1.55 (s, 9H). ^{13}C NMR (100 MHz, $CDCl_3$, 25 °C) δ: 163.9, 158.7, 148.5, 136.7, 126.0, 121.6, 81.8, 27.8, 24.3. HR-ESI-MS calcd for $[C_{11}H_{15}NO_2 + H]^+$: 194.1181; found: 194.1183, $[M + H]^+$, PPM = 1.0.

***tert*-Butyl 6-(bromomethyl)picolinate (2).** Compound **1** (1.82 g, 9.45 mmol) was dissolved in CCl_4 (15 mL), followed by addition of *N*-bromosuccinimide (NBS, 1.18 g, 6.62 mmol) and benzoyl peroxide (Bz_2O_2, 0.2 g, ~10 wt%). The reaction mixture was brought to reflux for 4 h, removed from heat and allowed

to cool to room temperature, filtered through a fritted glass filter, reduced to dryness *in vacuo*, resuspended in CH_2Cl_2, again filtered through a fritted glass filter and reduced to dryness. The crude product was purified by silica chromatography (CombiFlash R_f automated column system; 80 g HP silica; A: hexanes, B: ethyl acetate, 100% A to 75% A gradient) to yield the product **2** as a waxy faint-yellow solid (40%, ~1.04 g) (R_f: 0.4, TLC in 75% hexanes : 25% ethyl acetate). In addition, ~1.15 g of starting material was recovered (R_f: 0.3, TLC in 75% hexanes : 25% ethyl acetate). The major byproduct observed was the dibrominated product (R_f: 0.5, TLC in 75% hexanes : 25% ethyl acetate). ^{1}H NMR (300 MHz, $CDCl_3$, 25 °C) δ: 7.86 (d, J = 7.1 Hz, 1H), 7.75 (t, J = 7.6 Hz, 1H), 7.57 (d, J = 7.1 Hz, 1H), 4.56 (s, 2H), 1.54 (s, 9H). ^{13}C NMR (75 MHz, $CDCl_3$, 25 °C) δ: 163.2, 157.0, 148.5, 137.8, 126.3, 123.7, 82.1, 33.1, 27.8. HR-ESI-MS calcd for $[C_{11}H_{14}NO_2Br + H]^+$: 272.0286; found: 272.0289, $[M + H]^+$, PPM = 1.1.

***N*,*N*′-(2-Nitrobenzenesulfonamide)-1,2-diaminoethane (3).** Compound **3** was prepared according to a literature procedure:[8] ethylenediamine (548 μL, 8.2 mmol) was dissolved in THF (10 mL) and the reaction vessel placed in an ice bath. Sodium bicarbonate (~2 g) was then added, followed by slow addition of 2-nitrobenzenesulfonyl chloride (4.00 g, 18.1 mmol). The reaction mixture was allowed to warm to ambient temperature and stirred overnight. The yellow mixture was filtered to remove sodium bicarbonate, reduced to dryness *in vacuo* to yield a red oil, and then dissolved in a minimum volume of dichloromethane and placed in the freezer overnight. The precipitated product was filtered and then washed with cold dichloromethane (3 × 10 mL). This process was repeated with the filtrate once more to recover more material. The faint yellow powder (**3**) was dried *in vacuo* for a yield of 87% (~3.07 g). ^{1}H NMR (300 MHz, DMSO-d_6, 25 °C) δ: 8.16 (br s, 2H), 8.00–7.94 (m, 4H), 7.90–7.83 (m, 4H), 3.00 (s, 4H). ^{13}C NMR (75 MHz, DMSO-d_6, 25 °C) δ: 147.6, 134.2, 132.8, 132.4, 129.4, 124.5, 42.4. HR-ESI-MS calcd for $[C_{14}H_{14}N_4O_8S_2 + Na]^+$: 453.0151; found: 453.0154 $[M + Na]^+$, PPM = 0.7.

***N*,*N*′-(2-Nitrobenzenesulfonamide)-*N*,*N*′-[6-(*tert*-butoxycarbonyl)pyridin-2-yl]methyl]-1,2-diaminoethane (4).** To a solution of **3** (0.206 g, 0.479 mmol) in dimethylformamide (10 mL, dried over molecular sieves, 4 Å) was added **2** (0.391 g, 1.44 mmol) and sodium carbonate (~1 g). The faint yellow reaction mixture was stirred at 80 °C for 48 h, filtered to remove sodium carbonate, and concentrated *in vacuo*. The separation of the mono- and di-alkylated products was very difficult, and so the reaction was left until as complete as possible. The crude product was purified by silica chromatography (CombiFlash R_f automated column system; 40 g HP silica; A: hexanes, B: ethyl acetate, 100% A to 50% A slow gradient) to yield the product **4** as light yellow fluffy solid (55%, ~0.213 g) (R_f: 0.9, TLC in 95% dichloromethane : 5% MeOH). ^{1}H NMR (400 MHz, $CDCl_3$, 25 °C) δ: 8.18–8.16 (m, 2H), 7.86 (d, J = 7.6 Hz, 2H), 7.73 (t, J = 7.6 Hz, 2H), 7.69–7.62 (m, 4H), 7.60–7.56 (m, 2H), 7.50 (d, J = 7.6 Hz, 2H), 4.73 (s, 4H), 3.56 (s, 4H), 1.58 (s, 18H). ^{13}C NMR (100 MHz, $CDCl_3$, 25 °C) δ: 163.4, 156.1, 148.9, 147.9, 137.7, 133.5, 132.6, 132.1, 131.4, 125.3, 123.9, 123.7, 82.0, 53.3, 46.5, 28.0. HR-ESI-MS calcd for $[C_{36}H_{40}N_6O_{12}S_2 + Na]^+$: 835.2043; found: 835.2042, $[M + Na]^+$, PPM = −0.1.

***N*,*N*′-[6-(*tert*-Butoxycarbonyl)pyridin-2-yl]methyl-1,2-diaminoethane (5).** To a solution of **4** (0.234 g, 0.288 mmol) in tetrahydrofuran (5 mL) was added thiophenol (68 mL, 0.662 mmol) and potassium carbonate (excess, ~0.5 g). The reaction mixture was stirred at 50 °C for 48 h, during which time a colour change from colourless to dark yellow occurred. In Chapter 3, the potassium carbonate had become sticky during the course of the reaction, and would clog fritted glass filters, and so it was removed *via* centrifugation in 20 mL centrifuge tubes.[8,9] Here the crude reaction mixture was less sticky than previously found, and was filtered with a large fritted glass filter, rinsed liberally with THF and CH_3CN, and then concentrated to dryness *in vacuo*. The resulting crude yellow oil was purified by silica chromatography (CombiFlash R_f automated column system; 24 g neutral alumina; A: dichloromethane, B: methanol, 100% A to 75% A gradient) to yield **5** as clear colourless oil (80%, ~0.102 g). Compound **5** was purified using column chromatography on neutral alumina; silica should be avoided as **5** has a high affinity for silica and requires the use of ammonium hydroxide and >20% methanol for elution, giving partial *tert*-butyl ester deprotection and dissolution of some silica. ^{1}H NMR (400 MHz, $CDCl_3$, 25 °C) δ: 7.87 (d, J = 7.6 Hz, 2H), 7.74 (t, J = 7.6 Hz, 2H), 7.52 (d, J = 7.6 Hz, 2H), 4.00 (s, 4H), 2.81 (s, 4H), 2.26 (s, –N*H*–, 2H), 1.61 (s, 18H). ^{13}C NMR (100 MHz, $CDCl_3$, 25 °C) δ: 164.1, 160.5, 148.8, 137.1, 125.0, 122.9, 99.9, 81.9, 55.0, 49.0, 28.0. HR-ESI-MS calcd for $[C_{24}H_{34}N_4O_4 + K]^+$: 481.2217; found: 481.2213, $[M + K]^+$, PPM = −0.8.

H_2dedpa, *N*,*N*′-[(6-carboxylato)pyridin-2-yl)methyl]-1,2-diaminoethane (6). Compound **5** (49.3 mg, 0.114 mmol) was dissolved in a mixture of trifluoroacetic acid (TFA) (1 mL) and CH_2Cl_2 (1 mL) and stirred overnight at room temperature. The reaction mixture was concentrated *in vacuo* and then purified *via* semi-preparative reverse-phase HPLC (10 mL min^{-1}, gradient: A: 0.1% TFA in deionized water, B: 0.1% TFA in CH_3CN. 5% to 50% B linear gradient 30 min. t_R = 14.8 min, broad). Product fractions were pooled and lyophilized to a white powder overnight. The trifluoroacetic acid salt H_2dedpa·2 trifluoroacetic acid·1.5H_2O (**6**) was obtained as a white solid (~45 mg, 67% yield, using the molecular weight of the trifluoroacetic acid salt as determined by elemental analysis), with a cumulative yield of 26% over 4 steps. ^{1}H NMR (300 MHz, MeOD, 25 °C) δ: 8.19 (d, J = 7.7 Hz, 2H, pyr–*H*), 8.11 (t, J = 7.7 Hz, 2H, pyr–*H*), 7.76 (d, J = 7.8 Hz, 2H, pyr–*H*), 4.78 (s, 4H, Pyr–CH_2–N), 3.72 (s, 4H, ethylene–*H*). ^{13}C NMR (75 MHz, MeOD, 25 °C) δ: 167.8, 153.3, 148.6, 140.8, 127.7, 126.5, 50.9, 45.6. IR (neat, ATR-IR): ν = 1719 cm^{-1} (C═O), 1679/1591 cm^{-1} (C═C py). HR-ESI-MS calcd for $[C_{16}H_{18}N_4O_4 + H]^+$: 331.1406; found $[M + H]^+$: 331.1409, PPM = 0.9. Elemental analysis: calcd% for H_2dedpa·2CF_3COOH·1.5H_2O ($C_{16}H_{18}N_4O_4$·2CF_3COOH·1.5H_2O = 585.408): C 41.03, H 3.96, N 9.57; found: C 40.92 (Δ = 0.11), H 3.97 (Δ = 0.01), N 9.32 (Δ = 0.25).

***N,N′*-[(*tert*-Butoxycarbonyl)methyl-*N,N′*-[6-(*tert*-butoxycarbonyl)-pyridin-2-yl]methyl]-1,2-diaminoethane (7).** To a solution of **5** (22.8 mg, 0.0515 mmol) in acetonitrile (5 mL) was added *tert*-butylbromoacetate (18.3 μL, 0.124 mmol) and sodium carbonate (~300 mg). The reaction mixture was stirred at 60 °C for 48 h. Sodium carbonate was removed by filtration and the crude reaction mixture was concentrated *in vacuo*. The crude oil was purified by column chromatography (CombiFlash R_f automated column system; 40 g HP silica; A: dichloromethane, B: methanol, 100% A to 80% A gradient) to afford the product **7** as light yellow oil (96%, ~33.2 mg) (R_f: 0.65, TLC in 80% dichloromethane: 20% MeOH). ^{1}H NMR (400 MHz, $CDCl_3$, 25 °C) δ: 7.90–7.89 (m, 4H), 7.55–7.53 (m, 2H), 3.86 (s, 4H), 3.05 (s, 4H), 2.68 (s, 4H), 1.50 (s, 18H), 1.33 (s, 18H). ^{13}C NMR (100 MHz, $CDCl_3$, 25 °C) δ: 171.6, 163.8, 158.1, 148.1, 138.7, 126.7, 123.5, 82.9, 82.0, 60.5, 56.1, 53.3, 27.8. HR-ESI-MS calcd for $[C_{36}H_{54}N_4O_8 + H]^+$: 671.4020; found: 671.4019, $[M + H]^+$, PPM = −0.1.

H_4octapa, *N,N′*-[(6-carboxylato)pyridin-2-yl)methyl]-*N,N′*-diacetic acid-1,2-diaminoethane (8). Compound **7** (33.2 mg, 0.0495 mmol) was dissolved in a mixture of trifluoroacetic acid (TFA) (1 mL) and CH_2Cl_2 (1 mL) and stirred overnight at room temperature. The reaction mixture was concentrated *in vacuo* and then purified *via* semi-preparative reverse-phase HPLC (10 mL min^{-1}, gradient: A: 0.1% TFA in deionized water, B: 0.1% TFA in CH_3CN. 5% to 50% B linear gradient 30 min. t_R = 14.8 min, broad). Product fractions were pooled and lyophilized to a white powder overnight. The trifluoroacetic acid salt H_4octapa·2trifluoroacetic acid (**8**) was obtained as white solid (~45 mg, 74% yield, using the molecular weight of the trifluoroacetic acid salt as determined by elemental analysis), with a cumulative yield of ~27% over 5 steps. ^{1}H NMR (300 MHz, MeOD, 25 °C) δ: 8.04 (d, J = 7.6, 2H, pyr–*H*), 7.95 (t, J = 7.7, 2H, pyr–*H*), 7.63 (d, J = 7.5, 2H, pyr–*H*), 4.59 (s, 4H, Pyr–C*H*$_2$–N), 4.07 (s, 4H, HOOC–C*H*$_2$–N), 3.63 (s, 4H, ethylene–*H*). ^{13}C NMR (75 MHz, MeOD, 25 °C) δ: 171.8, 167.4, 156.7, 148.9, 140.0, 128.6, 125.8, 58.9, 56.0, 52.3. IR (neat, ATR-IR): ν = 1687/1672 cm^{-1} (C═O), 1618/1594 cm^{-1} (C═C py). HR-ESI-MS calcd for $[C_{20}H_{22}N_4O_8 + H]^+$: 447.1516; found $[M + H]^+$: 447.1515, PPM = −0.2. Elemental analysis: calcd% for H_4octapa·2CF_3COOH ($C_{20}H_{22}N_4O_8$·2CF_3COOH = 674.457): C 42.74, H 3.59, N 8.31; found: C 42.51 (Δ = 0.23), H 3.69 (Δ = 0.10), N 8.38 (Δ = 0.07).

[Na][Y(octapa)] (9). H_4octapa (**8**) (10 mg, 0.015 mmol) was suspended in 0.1 M HCl (1.0 mL) and YCl_3·6H_2O (5.5 mg, 0.018 mmol) was added. The pH was adjusted to ~4.0–4.5 using 0.1 M NaOH and then the solution was stirred at room temperature. After 1 hour the product was confirmed *via* mass spectrometry and the solvent was removed *in vacuo* to yield [Na][Y(octapa)] (**9**). ^{1}H NMR (400 MHz, D_2O, 25 °C) δ: 8.11–7.99 (m, 4H), 7.75–7.61 (m, 2H), 4.34–4.30 (m, 1H), 4.10–4.06 (m, 1H), 3.94 (m, 1H), 3.80–3.77 (m, 1H) 3.62 (m, 1H), 3.49–3.26 (m, 2H), 3.16 (m, 2H), 2.95–2.94 (m, 1H), 2.48–2.45 (m, 1H), 2.14–2.13 (m, 1H). ^{1}H NMR (300 MHz, DMSO-d_6, 25 °C) δ: 8.12–7.48 (m, 4H), 7.60–7.28 (m, 2H), 4.50–3.80 (m, 6H), 3.25–2.50 (m, 6H). ^{13}C NMR (150 MHz, DMSO-d_6, 25 °C) δ: 176.2, 168.8, 168.5, 168.2, 158.7, 157.5, 156.3, 155.7, 152.9, 152.8, 152.3, 141.5, 140.8, 140.4, 131.2, 130.5, 129.2, 124.7, 124.3, 124.1, 123.7, 122.9, 122.7, 122.6, 122.6, 122.4, 82.4, 62.9, 62.5, 62.1, 58.2, 56.9, 55.0, 53.7, 47.9, 40.0. HR-ESI-MS calcd for $[C_{20}H_{18}{}^{89}YN_4O_8 + 2Na]^+$: 576.9979; found: 576.9966, $[M + 2Na]^+$, PPM = −2.2.

1-(*p*-Nitrobenzyl)ethylenediamine (10). Compound **10** was prepared according to a literature procedure,[60] and was purified with a modified procedure using column chromatography (CombiFlash R_f automated column system; 40 g HP silica, A: 95% dichloromethane 5% ammonium hydroxide, B: 95% methanol 5% ammonium hydroxide, 100% A to 30% B gradient) to afford a **10** as brown/amber oil in a cumulative yield of 40% over 3 steps. ^{1}H NMR (300 MHz, $CDCl_3$, 25 °C) δ: 7.91 (d, J = 8.9 Hz, 2H), 7.18 (d, J = 8.5 Hz, 2H), 2.80–2.57 (m, 3H), 2.45–2.31 (m, 2H). ^{13}C NMR (75 MHz, $CDCl_3$, 25 °C) δ: 147.1, 147.7, 129.4, 122.8, 54.2, 47.5, 41.4. HR-ESI-MS calcd for $[C_9H_{13}N_3O_2 + H]^+$: 196.1086; found: 196.1084 [M + H], PPM = −1.0.

***N,N′*-(2-Nitrobenzenesulfonamide)-1-(*p*-nitrobenzyl)-1,2-diaminoethane (11).** Compound **11** was prepared according to a literature procedure.[8] Briefly, **10** (578 mg, 2.96 mmol) was dissolved in THF (10 mL) in a round bottom flask and placed in an ice bath, then sodium bicarbonate (~2 g) was added, followed by slow addition of 2-nitrobenzenesulfonyl chloride (1.58 g, 7.1 mmol). The reaction mixture was heated to 50 °C and stirred overnight. The yellow/orange mixture was filtered to remove sodium bicarbonate, rotary evaporated to an orange oil, dissolved in a minimum volume of dichloromethane and then placed in the freezer. The precipitated product was filtered and then washed with cold dichloromethane (3 × 10 mL); this process was repeated with the filtrate twice more to recover more product. The faint yellow powder (**11**) was dried *in vacuo* for a yield of 74% (~1.24 g) (R_f: 0.90, TLC in 10% methanol in dichloromethane). ^{1}H NMR (300 MHz, acetone-d_6, 25 °C) δ: 8.18–8.15 (m, 1H), 7.99–7.94 (m, 2H), 7.79–7.57 (m, 5H), 7.33 (d, J = 8.5 Hz, 2H), 7.04–6.98 (m, 2H), 4.01 (br s, 1H), 3.41–3.38 (m, 2H), 3.26 (dd, J = 3.4, 13.7 Hz, 1H), 2.98 (m, 1H). ^{13}C NMR (75 MHz, acetone-d_6, 25 °C) δ: 206.3, 149.2, 148.1, 147.6, 146.7, 135.2, 134.8, 134.2, 133.9, 133.8, 133.6, 131.7, 131.4, 130.9, 126.0, 125.7, 123.9, 57.7, 49.3, 38.2. HR-ESI-MS calcd for $[C_{21}H_{19}N_5O_{10}S_2 + Na]^+$: 588.0471; found: 588.0465 $[M + Na]^+$, PPM = −1.0.

***N,N′*-(2-Nitrobenzenesulfonamide)-*N,N″*-[6-(methoxycarbonyl)-pyridin-2-yl]methyl]-1-(*p*-nitrobenzyl)-1,2-diaminoethane (12).** To a solution of **11** (188 mg, 0.332 mmol) in dimethylformamide (5 mL, dried over molecular sieves, 4 Å) was added **2** (225.8 mg, 0.830 mmol) and sodium carbonate (~0.5 g). The yellow reaction mixture was stirred at 80 °C for 48 h, over which time the colour slowly changed to red. The reaction mixture was filtered to remove sodium carbonate and concentrated *in vacuo*. As with the analogous compound **4**, chromatographic separation of the mono- and di-alkylated product was very difficult, with the R_f difference being ~0.1 in 50 : 50 hexanes–ethyl acetate. The crude product was purified by silica chromatography (CombiFlash R_f automated column

system; 40 g HP silica; A: hexanes, B: ethyl acetate, 100% A to 50% A gradient) to yield **12** as faint yellow solid (81%, ~255 mg) (R_f = 0.65 in 50 : 50 EtOAc–Hex). ^{1}H NMR (300 MHz, $CDCl_3$, 25 °C) δ: 8.00–7.83 (m, 4H), 7.78–7.60 (m, 7H), 7.59–7.7.42 (m, 4H), 7.38–7.21 (m, 1H), 7.01 (d, J = 9 Hz, 2H), 4.97–4.65 (m, 4H), 4.36–4.29 (m, 1 H), 3.40–3.24 (m, 2H), 3.20–3.11 (m, 1H), 3.00–2.93 (m, 1H), 1.58 (s, 9H), 1.56 (s, 9H). ^{13}C NMR (75 MHz, $CDCl_3$, 25 °C) δ: 163.5, 163.2, 157.5, 155.9, 148.7, 148.6, 147.7, 146.9, 146.1, 144.7, 137.9, 137.7, 133.7, 133.3, 132.5, 132.3, 132.1, 132.0, 131.4, 129.6, 126.5, 125.3, 124.0, 123.9, 123.8, 123.8, 122.9, 82.2, 82.1, 57.8, 53.0, 51.4, 49.8, 34.4, 27.9. HR-ESI-MS calcd for $[C_{43}H_{45}N_7O_{14}S_2 + Na]^+$: 970.2364; found: 970.2355, $[M + Na]^+$, PPM = −0.9.

***N*,*N*′-[[6-(Methoxycarbonyl)pyridin-2-yl]methyl]-1-(*p*-nitrobenzyl)-1,2-diaminoethane (13).** To a solution of **12** (125 mg, 0.132 mmol) in tetrahydrofuran (5 mL) was added thiophenol (31 μL, 0.304 mmol) and potassium carbonate (excess, ~300 mg). The reaction mixture was stirred at 60 °C for 48 h, over which time the colour slowly changed from colourless to dark yellow. The crude reaction mixture was filtered with a fritted glass filter, rinsed *ad libitum* with THF and CH_3CN, and then concentrated to dryness *in vacuo*. The resulting crude yellow oil was purified by neutral alumina column chromatography (CombiFlash R_f automated column system; 24 g neutral alumina; A: dichloromethane, B: methanol, 100% A to 75% A gradient) to yield **13** as light yellow oil (70%, ~76 mg). ^{1}H NMR (400 MHz, $CDCl_3$, 25 °C) δ: 8.09 (d, J = 8.9 Hz, 2H), 7.86 (d, J = 7.9 Hz, 2H), 7.74–7.69 (m, 2H), 7.46 (t, J = 8.6 Hz, 2H), 7.34 (d, J = 8.5 Hz, 2H), 4.06–3.88 (m, 4H), 3.01–2.96 (m, 2H), 2.88–2.82 (m, 1H), 2.69–2.66 (m, 1H), 2.56–2.52 (m, 1H), 1.60 (s, 18H). ^{13}C NMR (100 MHz, $CDCl_3$, 25 °C) δ: 163.9, 163.9, 160.4, 148.7, 148.6, 147.3, 146.4, 137.2, 137.1, 130.1, 125.1, 125.0, 123.4, 122.9, 81.9, 58.3, 54.9, 52.4, 51.7, 39.2. HR-ESI-MS calcd for $[C_{31}H_{39}N_5O_6 + H]^+$: 578.2979; found: 578.2984, $[M + H]^+$, PPM = 0.9.

***p*-SCN-Bn-H$_2$dedpa, *N*,*N*′-[[(6-carboxylato)pyridin-2-yl]methyl]-1-(*p*-benzylisothiocyanato)-1,2-diaminoethane (14).** Compound **13** (43.1 mg, 0.0746 mmol) was dissolved in glacial acetic acid (2.5 mL) with hydrochloric acid (2.5 mL, 3 M), palladium on carbon (20 wt%), and hydrogen gas (balloon). The reaction mixture was stirred vigorously at rt for 1 hour, then filtered to remove Pd/C and washed *ad libitum* with acetonitrile and hydrochloric acid (3 M). The product was confirmed by low-resolution mass spectrometry (LRMS), and revealed that the *tert*-butyl ester protecting groups remained intact. The crude product was dissolved in HCl (2–3 mL, 3 M), and heated with a heat gun for 1 minute. Following this heating step, quantitative removal of the *tert*-butyl ester protecting groups was confirmed by LRMS. Without purification, the crude reaction mixture (in 2–3 mL of 3 M HCl) was reacted with thiophosgene (suspension in chloroform) in ~0.2 mL of additional chloroform (~86 μL, 1.12 mmol) overnight at ambient temperature with vigorous stirring. The reaction mixture was washed with chloroform (5 × 1 mL) by vigorous biphasic stirring, followed by decanting of the organic phase with a pipette to remove excess thiophosgene, diluted to a volume of 4.5 mL with deionized water, and injected directly onto a semi-preparative HPLC column for purification (A: 0.1% TFA in deionized water, B: 0.1% TFA in CH_3CN, 95% A to 60% B gradient over 40 min). *p*-SCN-Bn-H$_2$dedpa·2trifluoroacetic acid·H$_2$O (**14**) was found in the largest peak at R_t = 29 min, lyophilized overnight, and was isolated as a white solid (~23 mg, 43% over 3 steps from **13**, using the molecular weight of the trifluoroacetic acid salt as determined by elemental analysis). ^{1}H NMR (400 MHz, MeOD, 25 °C) δ: 8.18–8.08 (m, 4H), 7.77–7.72 (m, 2H), 7.36 (d, J = 8.5 Hz, 2H), 7.23 (m, J = 8.5 Hz, 2H), 4.95–4.84 (m, 3H), 4.68 (d, J = 16.7 Hz, 1H), 4.03–3.97 (m, 1H), 3.71–3.65 (m, 1H), 3.52–3.47 (m, 2H), 3.01–2.95 (m, 1H). ^{13}C NMR (100 MHz, MeOD, 25 °C) δ: 167.7, 167.6, 153.9, 153.5, 153.3, 148.4, 140.9, 140.3, 137.7, 135.5, 132.3, 132.2, 132.0, 130.6, 127.7, 127.4, 127.3, 126.6, 126.5, 59.8, 59.5, 50.7, 35.8. IR (neat, ATR-IR): ν = 2097 cm^{-1} (S═C═N–), 1665 cm^{-1} (C═O), 1594 cm^{-1} (C═C py). HR-ESI-MS calcd for $[C_{24}H_{23}N_5O_4S + H]^+$: 478.1549; found $[M + H]^+$: 478.1548, PPM = −0.2. Elemental analysis: calcd% for *p*-SCN-Bn-H$_2$dedpa·2CF$_3$COOH·1H$_2$O ($C_{24}H_{23}N_5O_4S$·2CF$_3$COOH·1H$_2$O = 723.597): C 46.48, H 3.76, N 9.68; found: C 46.68 (Δ = 0.20), H 3.73 (Δ = 0.03), N 9.60 (Δ = 0.08).

***N*,*N*′-[(*tert*-Butoxycarbonyl)methyl]-*N*,*N*′-[[(6-*tert*-butoxycarbonyl)pyridin-2-yl]methyl]-1-(*p*-nitrobenzyl)-1,2-diaminoethane (15).** To a solution of **13** (78.1 mg, 0.135 mmol) in acetonitrile (15 mL) was added *tert*-butylbromoacetate (~48 μL, 0.324 mmol) and potassium carbonate (~500 mg). The reaction mixture was stirred at 80 °C for 48 h. Potassium carbonate was removed by filtration and the crude reaction mixture was concentrated *in vacuo*. The crude oil was purified by column chromatography (CombiFlash R_f automated column system; 24 g HP silica; A: dichloromethane, B: methanol, 100% A to 80% A gradient) to afford the product **15** as light yellow oil (63%, ~69 mg) (R_f = 0.61 in 80 : 20 CH_2Cl_2–MeOH). ^{1}H NMR (400 MHz, $CDCl_3$, 25 °C) δ: 8.02–7.97 (m, 3H), 7.89–7.73 (m, 3H), 7.64–7.60 (m, 1H), 7.56–7.46 (m, 3H), 4.03–3.93 (m, 4H), 3.43–3.21 (m, 4H), 3.03–2.95 (m, 2H), 2.86–2.81 (m, 2H), 2.50–2.45 (m, 1H), 1.62 (m, 18H), 1.46 (m, 18H). ^{13}C NMR (100 MHz, $CDCl_3$, 25 °C) δ: 170.6, 170.5, 163.9, 160.2, 160.1, 148.7, 148.6, 148.2, 146.2, 136.9, 136.9, 130.2, 126.1, 125.6, 123.4, 123.2, 123.1, 82.0, 81.9, 81.1, 80.9, 61.4, 60.8, 56.9, 56.6, 54.1, 52.4, 35.7, 29.6, 28.1, 28.1, 28.0. HR-ESI-MS calcd for $[C_{43}H_{59}N_5O_{10} + H]^+$: 806.4340; found: 806.4339, $[M + H]^+$, PPM = −0.1.

***p*-SCN-Bn-H$_4$octapa, *N*,*N*′-[(Carboxylato)methyl]-*N*,*N*′-[[(6-carboxylato)pyridin-2-yl]methyl]-1-(*p*-benzylisothiocyanato)-1,2-diaminoethane (16).** Compound **15** (59.6 mg, 0.0739 mmol) was dissolved in glacial acetic acid (2.5 mL) with hydrochloric acid (2.5 mL, 3 M), palladium on carbon (30 wt%), and hydrogen gas (balloon). The reaction mixture was stirred vigorously at rt for 1 hour, filtered to remove Pd/C and washed *ad libitum* with acetonitrile and hydrochloric acid (3 M). The product was confirmed by low-resolution mass spectrometry (LRMS), and revealed that two of the *tert*-butyl ester protecting groups remained intact and two had been removed. The crude product was dissolved in HCl (2–3 mL, 3 M), and heated with a heat gun for 1 minute to effect full ester deprotection. Follow-

ing heating, quantitative removal of the *tert*-butyl ester protecting groups was confirmed by LRMS. Without purification, the crude reaction mixture (in 2–3 mL of 3 M HCl) was reacted with thiophosgene (suspension in chloroform) in ~0.2 mL of additional chloroform (~85 μL, 1.11 mmol) overnight at ambient temperature with vigorous stirring. The reaction mixture was washed with chloroform (5 × 1 mL) by vigorous biphasic stirring followed by decanting of the organic phase with a pipette to remove excess thiophosgene, diluted to a volume of 4.5 mL with deionized water, and injected directly onto a semi-preparative HPLC column for purification (A: 0.1% TFA in deionized water, B: 0.1% TFA in CH_3CN, 100% A to 40% A gradient over 40 min). *p*-SCN-Bn-H_4octapa·2trifluoroacetic acid·0.5H_2O·0.5CH_3CN (**16**) was found in the largest peak at R_t = 34.5 min, lyophilized overnight, and was isolated as a white solid (~11 mg, 25% over 3 steps from **15**, using the molecular weight of the trifluoroacetic acid salt as determined by elemental analysis). ^{1}H NMR (400 MHz, MeOD, 25 °C) δ: 8.03–7.90 (m, 4H), 7.61–7.56 (m, 2H), 7.21–7.11 (m, 4H), 5.07 (m, 2H), 4.70 (m, 2H), 4.52–4.48 (m, 2H), 4.16–4.13 (m, 1H), 4.00–3.94 (m, 2H), 3.68–3.57 (m, 2H), 3.25–3.20 (m, 1H), 2.68–2.62 (m, 1H). ^{13}C NMR (150 MHz, MeOD, 25 °C) δ: 174.5, 169.3, 167.8, 167.4, 167.2, 160.8, 152.7, 149.1, 148.6, 140.0, 139.9, 138.9, 131.8, 131.7, 131.1, 129.2, 128.0, 127.0, 126.1, 125.3, 125.1, 61.1, 55.5, 52.1, 50.7, 38.1, 34.7. IR (neat, ATR-IR): ν = 2096 cm^{-1} (S═C═N–), 1703/1660 cm^{-1} (C═O), 1593 cm^{-1} (C═C py). HR-ESI-MS calcd for $[C_{28}H_{27}N_5O_8S + H]^+$: 594.1659; found $[M + H]^+$: 594.1650, PPM = −1.5. Elemental analysis: calcd% for *p*-SCN-Bn-H_4octapa·2CF_3COOH·0.5H_2O·0.5CH_3CN ($C_{28}H_{27}N_5O_8S$ ·2CF_3COOH·0.5H_2O·0.5CH_3CN = 851.188): C 46.57, H 3.73, N 9.05; found: C 46.92 (Δ = 0.35), H 4.00 (Δ = 0.27), N 8.67 (Δ = 0.38).

Solution thermodynamics

The experimental procedures and details of the apparatus closely followed our reported studies of H_2dedpa/Ga^{3+}, and H_4octapa with In^{3+} and Lu^{3+}.[7,8,36] As a result of the strength of the binding of the Y^{3+} complex $[Y(octapa)]^-$, the complex formation constant with this ligand could not be determined directly and ligand–ligand competition using Na_2H_2EDTA was used. Potentiometric titrations were performed using a Metrohm Titrando 809 equipped with a Ross combination pH electrode and a Metrohm Dosino 800. Data were collected in triplicate using PC Control (Version 6.0.91, Metrohm). The titration apparatus consisted of a water-jacketed glass vessel maintained at 25.0 (±0.1 °C, Julabo water bath). Prior to and during the course of the titration, a blanket of nitrogen, passed through 10% NaOH to exclude any CO_2, was maintained over the sample solution. Yttrium ion solutions were prepared by dilution of the appropriate atomic absorption standard (AAS) solution. The exact amount of acid present in the yttrium standard was determined by titration of an equimolar solution of Y^{3+} and Na_2H_2EDTA. The amount of acid present was determined by Gran's method.[61] Calibration of the electrode was performed prior to each measurement by titrating a known amount of HCl with 0.1 M NaOH. Calibration data were analyzed by standard computer treatment provided within the program MacCalib[62] to obtain the calibration parameters E_0. Ligand solutions were prepared 24 hours in advance of titrations to allow for equilibration. Electrode equilibration times for titrations were up to 10 min for pK_a titrations and up to 3 h for metal complex titrations (<0.2 mV min^{-1} drift allowed). Ligand and metal concentrations were 0.75–1.0 mM for potentiometric titrations. The data were treated with Hyperquad2008.[63] The proton dissociation constants corresponding to hydrolysis of $Y^{3+}_{(aq)}$ ion included in the calculations were taken from Baes and Mesmer.[52] The K_{ML} value for the yttrium-EDTA complex was taken from Martell.[51] It was necessary to include a ML(OH) species in the equilibrium model used for fitting where log $K_{ML(OH)}$ = 10.6(1). This is consistent with a 9-coordinate structure and only becomes relevant above pH 9.5. Values of pM were calculated at physiologically relevant conditions of pH 7.4, 10 μM ligand, and 1 μM metal. All values and errors represent the average of at least three independent experiments.

Molecular modeling

Calculations were performed using the Gaussian 09[64] and GaussView packages. Molecular geometries and electron densities were obtained from density functional theory calculations, with the B3LYP functional employing the 6-31+G(d,p) basis set for 1st and 2nd row elements and the Stuttgart–Dresden effective core potential, SDD for yttrium.[65–67] Solvent (water) effects were described through a continuum approach by means of the IEF PCM as implemented in G09. The electrostatic potential was mapped onto the calculated electron density surface. The corresponding harmonic vibration frequencies were computed at the same level to characterize the geometry as a minima.

Acknowledgements

We acknowledge NSERC for CGS-M/CGS-D fellowships (E.W.P.) and many years of research support (C.O.), as well as the University of British Columbia for a 4YF fellowship (E.W.P.). C.O. acknowledges the Canada Council for the Arts for a Killam Research Fellowship (2011–2013) and the Alexander von Humboldt Foundation for a Research Award, as well as Prof. Dr Peter Comba and his research group in Heidelberg for hospitality and interesting discussions.

Notes and references

1 E. W. Price and C. Orvig, *Chem. Soc. Rev.*, 2014, **43**, 260–290.
2 T. J. Wadas, E. H. Wong, G. R. Weisman and C. J. Anderson, *Chem. Rev.*, 2010, **110**, 2858–2902.
3 C. F. Ramogida and C. Orvig, *Chem. Commun.*, 2013, **49**, 4720–4739.

4 B. M. Zeglis and J. S. Lewis, *Dalton Trans.*, 2011, **40**, 6168–6195.
5 J. P. Holland, M. J. Williamson and J. S. Lewis, *Mol. Imaging*, 2010, **9**, 1–20.
6 G. A. Bailey, E. W. Price, B. M. Zeglis, C. L. Ferreira, E. Boros, M. J. Lacasse, B. O. Patrick, J. S. Lewis, M. J. Adam and C. Orvig, *Inorg. Chem.*, 2012, **51**, 12575–12589.
7 E. W. Price, J. F. Cawthray, G. A. Bailey, C. L. Ferreira, E. Boros, M. J. Adam and C. Orvig, *J. Am. Chem. Soc.*, 2012, **134**, 8670–8683.
8 E. W. Price, B. M. Zeglis, J. F. Cawthray, C. F. Ramogida, N. Ramos, J. S. Lewis, M. J. Adam and C. Orvig, *J. Am. Chem. Soc.*, 2013, **135**, 12707–12721.
9 E. W. Price, B. M. Zeglis, J. S. Lewis, M. J. Adam and C. Orvig, *Dalton Trans.*, 2014, **43**, 119–131.
10 R. Weiner and M. Thakur, *BioDrugs*, 2005, **19**, 145–163.
11 F. Forrer, C. Waldherr, H. R. Maecke and J. Mueller-Brand, *Anticancer Res.*, 2006, **26**, 703–707.
12 F. Forrer, H. Uusijärvi, D. Storch, H. R. Maecke and J. Mueller-Brand, *J. Nucl. Med.*, 2005, **46**, 1310–1316.
13 T. K. Nayak, K. Garmestani, D. E. Milenic, K. E. Baidoo and M. W. Brechbiel, *PLoS One*, 2011, **6**, e18198.
14 T. K. Nayak, K. Garmestani, K. E. Baidoo, D. E. Milenic and M. W. Brechbiel, *Int. J. Cancer*, 2010, **128**, 920–926.
15 S. Palm, R. M. Enmon, C. Matei, K. S. Kolbert, S. Xu, P. B. Zanzonico, R. L. Finn, J. A. Koutcher, S. M. Larson and G. Sgouros, *J. Nucl. Med.*, 2003, **44**, 1148–1155.
16 L. I. Gordon, T. E. Witzig, G. A. Wiseman, I. W. Flinn, S. S. Spies, D. H. Silverman, C. Emmanuolides, L. Cripe, M. Saleh, M. S. Czuczman, T. Olejnik, C. A. White and A. J. Grillo-López, *Semin. Oncol.*, 2002, **29**, 87–92.
17 M. F. Giblin, B. Veerendra and C. J. Smith, *In Vivo*, 2005, **19**, 9–29.
18 H. Herzog, F. Rösch, G. Stöcklin, C. Lueders, S. M. Qaim and L. E. Feinendegen, *J. Nucl. Med.*, 1993, **34**, 2222–2226.
19 H.-S. Chong, K. Garmestani, D. Ma, D. E. Milenic, T. Overstreet and M. W. Brechbiel, *J. Med. Chem.*, 2002, **45**, 3458–3464.
20 H.-S. Chong, H. A. Song, X. Ma, D. E. Milenic, E. D. Brady, S. Lim, H. Lee, K. Baidoo, D. Cheng and M. W. Brechbiel, *Bioconjugate Chem.*, 2008, **19**, 1439–1447.
21 C. S. Kang, X. Sun, F. Jia, H. A. Song, Y. Chen, M. Lewis and H.-S. Chong, *Bioconjugate Chem.*, 2012, **23**, 1775–1782.
22 L. Camera, S. Kinuya, K. Garmestani, C. Wu, M. W. Brechbiel, L. H. Pai, T. J. McMurry, O. A. Gansow, I. Pastan, C. H. Paik and J. A. Carrasquillo, *J. Nucl. Med.*, 1994, **35**, 882–889.
23 G. J. Förster, M. J. Engelbach, J. J. Brockmann, H. J. Reber, H. G. Buchholz, H. R. Mäcke, F. R. Rösch, H. R. Herzog and P. R. Bartenstein, *Eur. J. Nucl. Med.*, 2001, **28**, 1743–1750.
24 C. Wu, H. Kobayashi, B. Sun, T. M. Yoo, C. H. Paik, O. A. Gansow, J. A. Carrasquillo, I. Pastan and M. W. Brechbiel, *Bioorg. Med. Chem.*, 1997, **5**, 1925–1934.
25 M. W. Brechbiel, O. A. Gansow, R. W. Atcher, J. Schlom, J. Esteban, D. Simpson and D. Colcher, *Inorg. Chem.*, 1986, **25**, 2772–2781.
26 A. Harrison, C. A. Walker, D. Parker, K. J. Jankowski, J. P. L. Cox, A. S. Craig, J. M. Sansom, N. R. A. Beeley, R. A. Boyce, L. Chaplin, M. A. W. Eaton, A. P. H. Farnsworth, K. Millar, A. T. Millican, A. M. Randall, S. K. Rhind, D. S. Secher and A. Turner, *Int. J. Radat. Appl. Instrum., Part B*, 1991, **18**, 469–476.
27 C. A. Boswell and M. W. Brechbiel, *Nucl. Med. Biol.*, 2007, **34**, 757–778.
28 W. A. P. Breeman, M. de Jong, T. J. Visser, J. L. Erion and E. P. Krenning, *Eur. J. Nucl. Med. Mol. Imaging*, 2003, **30**, 917–920.
29 T. Clifford, C. A. Boswell, G. B. Biddlecombe, J. S. Lewis and M. W. Brechbiel, *J. Med. Chem.*, 2006, **49**, 4297–4304.
30 M. Cremonesi, M. Ferrari, S. Zoboli, M. Chinol, M. G. Stabin, F. Orsi, H. R. Maecke, E. Jermann, C. Robertson, M. Fiorenza, G. Tosi and G. Paganelli, *Eur. J. Nucl. Med. Mol. Imaging*, 1999, **26**, 877–886.
31 M. Gabriel, C. Decristoforo, D. Kendler, G. Dobrozemsky, D. Heute, C. Uprimny, P. Kovacs, E. Von Guggenberg, R. Bale and I. J. Virgolini, *J. Nucl. Med.*, 2007, **48**, 508–518.
32 M. Lin, M. Welch and S. Lapi, *Mol. Imaging Biol.*, 2013, **15**, 1–8.
33 S. Pauwels, R. Barone, S. Walrand, F. Borson-Chazot, R. Valkema, L. K. Kvols, E. P. Krenning and F. Jamar, *J. Nucl. Med.*, 2005, **46**, 92S–98S.
34 A. Romer, D. Seiler, N. Marincek, P. Brunner, M. T. Koller, Q. K. T. Ng, H. R. Maecke, J. Müller-Brand, C. Rochlitz, M. Briel, C. Schindler and M. A. Walter, *Eur. J. Nucl. Med. Mol. Imaging*, 2014, **41**, 214–222.
35 R. Kashyap, P. Jackson, M. S. Hofman, P. Eu, J.-M. Beauregard, D. Zannino and R. J. Hicks, *Eur. J. Nucl. Med. Mol. Imaging*, 2013, **40**, 1853–1860.
36 E. Boros, C. L. Ferreira, J. F. Cawthray, E. W. Price, B. O. Patrick, D. W. Wester, M. J. Adam and C. Orvig, *J. Am. Chem. Soc.*, 2010, **132**, 15726–15733.
37 A. Armstrong, I. Brackenridge, R. F. W. Jackson and J. M. Kirk, *Tetrahedron Lett.*, 1988, **29**, 2483–2486.
38 Y. Gultneh, B. Ahvazi, Y. T. Tesema, T. B. Yisgedu and R. J. Butcher, *J. Coord. Chem.*, 2006, **59**, 1835–1846.
39 E. Boros, C. L. Ferreira, D. T. T. Yapp, R. K. Gill, E. W. Price, M. J. Adam and C. Orvig, *Nucl. Med. Biol.*, 2012, **39**, 785–794.
40 E. Boros, J. F. Cawthray, C. L. Ferreira, B. O. Patrick, M. J. Adam and C. Orvig, *Inorg. Chem.*, 2012, **51**, 6279–6284.
41 R. Ferreiros-Martinez, D. Esteban-Gomez, C. Platas-Iglesias, A. d. Blas and T. Rodriguez-Blas, *Dalton Trans.*, 2008, 5754–5765.
42 E. Balogh, M. Mato-Iglesias, C. Platas-Iglesias, E. Toth, K. Djanashvili, J. A. Peters, A. de Blas and T. Rodriguez-Blas, *Inorg. Chem.*, 2006, **45**, 8719–8728.

43 C. Platas-Iglesias, M. Mato-Iglesias, K. Djanashvili, R. N. Muller, L. V. Elst, J. A. Peters, A. de Blas and T. Rodríguez-Blas, *Chem. – Eur. J.*, 2004, **10**, 3579–3590.
44 R. Shannon, *Acta Crystallogr., Sect. A: Cryst. Phys., Diffr., Theor. Gen. Cryst.*, 1976, **32**, 751–767.
45 E. T. Clarke and A. E. Martell, *Inorg. Chim. Acta*, 1991, **190**, 37–46.
46 W. R. Harris and V. L. Pecoraro, *Biochemistry*, 1983, **22**, 292–299.
47 K. N. Raymond, G. Müller and B. Matzanke, in *Topics in Current Chemistry*, ed. F. L. Boschke, Springer-Verlag, Berlin, Heidelberg, 1984, vol. 123, pp. 49–102.
48 M. J. Kappel and K. N. Raymond, *Inorg. Chem.*, 1982, **21**, 3437–3442.
49 M. Koudelková, H. Vinšová and V. Jedináková-Křížová, *J. Chromatogr. A*, 2003, **990**, 311–316.
50 K. Kumar, C. A. Chang, L. C. Francesconi, D. D. Dischino, M. F. Malley, J. Z. Gougoutas and M. F. Tweedle, *Inorg. Chem.*, 1994, **33**, 3567–3575.
51 A. E. Martell and R. M. Smith, *Critical Stability Constants*, Plenum Press, New York, 1974–1989, vol. 1–6.
52 C. F. Baes Jr. and R. E. Mesmer, *The Hydrolysis of Cations*, Wiley-Interscience, New York, 1976.
53 C. F. G. C. Geraldes, R. Delgado, A. M. Urbano, J. Costa, F. Jasanada and F. Nepveu, *J. Chem. Soc., Dalton Trans.*, 1995, 327–335.
54 É. Tóth and E. Brücher, *Inorg. Chim. Acta*, 1994, **221**, 165–167.
55 W. P. Cacheris, S. K. Nickle and A. D. Sherry, *Inorg. Chem.*, 1987, **26**, 958–960.
56 M. F. Loncin, J. F. Desreux and E. Merciny, *Inorg. Chem.*, 1986, **25**, 2646–2648.
57 C. J. Broan, J. P. L. Cox, A. S. Craig, R. Kataky, D. Parker, A. Harrison, A. M. Randall and G. Ferguson, *J. Chem. Soc., Perkin Trans. 2*, 1991, 87–99.
58 W. R. Harris, Y. Chen and K. Wein, *Inorg. Chem.*, 1994, **33**, 4991–4998.
59 W. R. Harris, B. Yang, S. Abdollahi and Y. Hamada, *J. Inorg. Biochem.*, 1999, **76**, 231–242.
60 A. Kumar Mishra, P. Panwar, M. Chopra, R. Kumar Sharma and J.-F. Chatal, *New J. Chem.*, 2003, **27**, 1054–1058.
61 G. Gran, *Analyst*, 1952, **77**, 661–671.
62 P. Duckworth, *Private communication*.
63 P. Gans, A. Sabatini and A. Vacca, *Talanta*, 1996, **43**, 1739–1753.
64 G. W. T. M. J. Frisch, H. B. Schlegel, G. E. Scuseria, M. A. Robb, J. R. Cheeseman, G. Scalmani, V. Barone, B. Mennucci, G. A. Petersson, H. Nakatsuji, M. Caricato, X. Li, H. P. Hratchian, A. F. Izmaylov, J. Bloino, G. Zheng, J. L. Sonnenberg, M. Hada, M. Ehara, K. Toyota, R. Fukuda, J. Hasegawa, M. Ishida, T. Nakajima, Y. Honda, O. Kitao, H. Nakai, T. Vreven, J. A. Montgomery Jr., J. E. Peralta, F. Ogliaro, M. Bearpark, J. J. Heyd, E. Brothers, K. N. Kudin, V. N. Staroverov, R. Kobayashi, J. Normand, K. Raghavachari, A. Rendell, J. C. Burant, S. S. Iyengar, J. Tomasi, M. Cossi, N. Rega, J. M. Millam, M. Klene, J. E. Knox, J. B. Cross, V. Bakken, C. Adamo, J. Jaramillo, R. Gomperts, R. E. Stratmann, O. Yazyev, A. J. Austin, R. Cammi, C. Pomelli, J. W. Ochterski, R. L. Martin, K. Morokuma, V. G. Zakrzewski, G. A. Voth, P. Salvador, J. J. Dannenberg, S. Dapprich, A. D. Daniels, Ö. Farkas, J. B. Foresman, J. V. Ortiz, J. Cioslowski and D. J. Fox, *GAUSSIAN 09 (Revision C.01)*, Gaussian, Inc., Wallingford, CT, 2010.
65 C. Lee, W. Yang and R. G. Parr, *Phys. Rev. B: Condens. Matter*, 1988, **37**, 785–789.
66 A. D. Becke, *J. Chem. Phys.*, 1993, **98**, 5648–5652.
67 X. Cao and M. Dolg, *J. Chem. Phys.*, 2001, **115**, 7348–7355.